

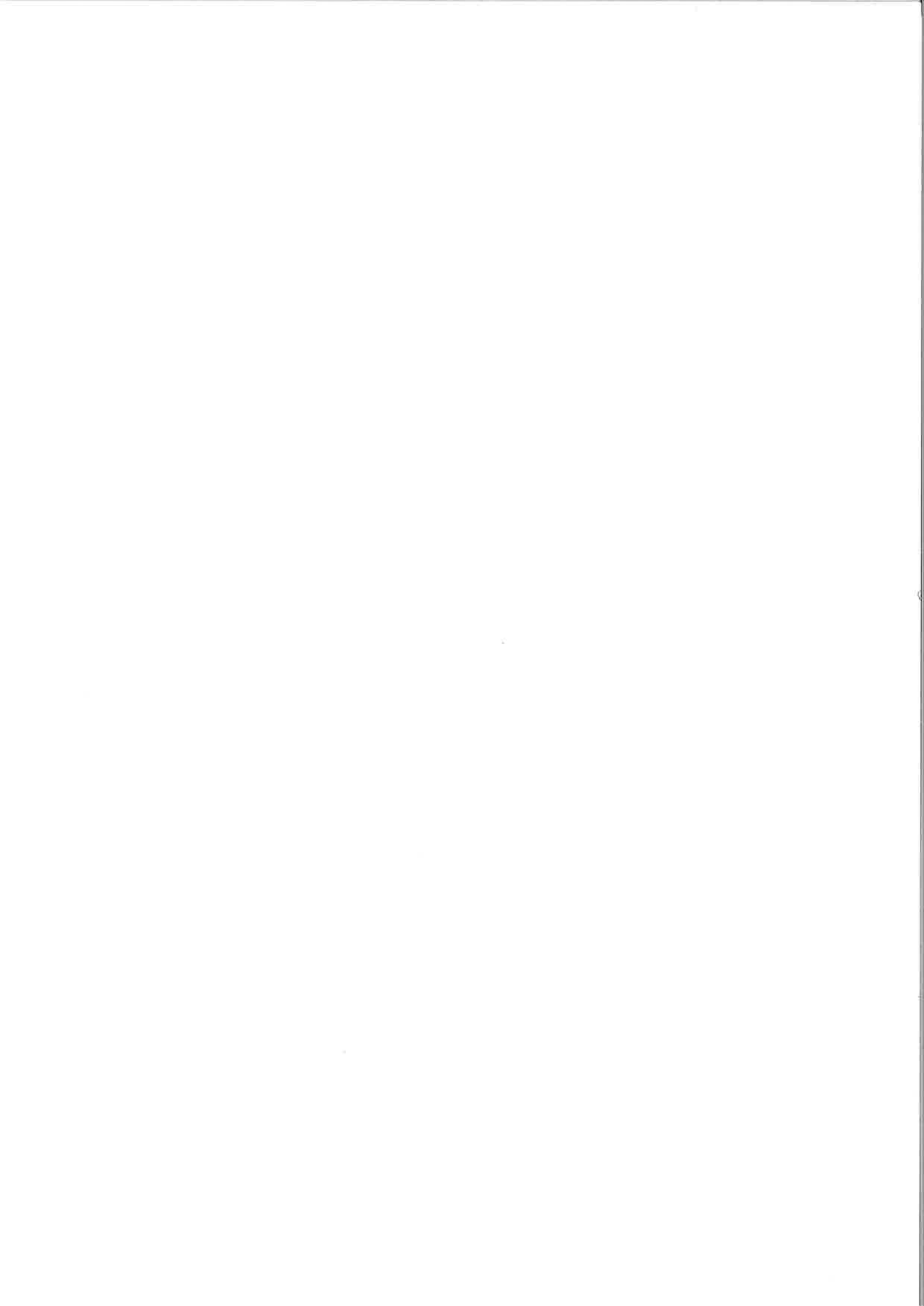
# **GEOLOGY FOR SOCIETY**

SINCE 1858



**GEOLOGICAL  
SURVEY OF  
NORWAY**

· NGU ·





|  |                                      |   |   |
|--|--------------------------------------|---|---|
| <b>Report no.:</b> 2018.012  |                                      | <b>ISSN: 0800-3416 (print)</b><br><b>ISSN: 2387-3515 (online)</b> | <b>Grading:</b> Open  |
| <b>Title:</b><br>Proposal for a new national radon hazard map - Trøndelag test area - COOP Project.                          |                                      |   |   |
| <b>Authors:</b><br>Torleif Lauritsen, Marie-Andrée Dumais, Frode Ofstad,<br>Odleiv Olesen, Trond Slagstad and Marco Brønner. |                                      | <b>Client:</b><br>Geological Survey of Norway.                    |   |
| <b>County:</b><br>Trøndelag  |                                      | <b>Commune:</b>   |   |
| <b>Map-sheet name (M=1:250.000)</b><br>Ålesund, Røros, Kristiansund, Trondheim, Østersund,<br>Namsos, Grong                  |                                      | <b>Map-sheet no. and -name (M=1:50.000)</b>                       |   |
| <b>Deposit name and grid-reference:</b>  |                                      | <b>Number of pages:</b> 45  | <b>Price (NOK):</b> 65,-  |
| <b>Fieldwork carried out:</b><br>1986-2015   | <b>Date of report:</b><br>19.02.2019 | <b>Project no.:</b><br>336600                                     | <b>Person responsible:</b><br> |

## Summary:

This report describes the work done to produce a radon hazard map for the Trøndelag county. It is our judgement that the techniques and types of data utilized, may also be used for preparation of a new national radon hazard map.

Earlier studies, in the Oslo area, have revealed the connection between the indoor radon concentrations and the airborne gamma ray eU (equivalent uranium) map. These studies consider airborne gamma ray survey eU data to be better than mapped geology at accounting for and therefore predicting differences in radon potential across the Oslo area. Based on this connection, we have used the following graduation of eU concentration in the ground (ppm) and radon hazard when introducing a radon map for Trøndelag: eU > 10 ppm is estimated as very high radon hazard, 3-10 ppm is considered high radon hazard, and eU < 3 ppm assumed as moderate to low radon hazard.

In COOP Phase 2, NGU has compiled both new surveys and existing radiometric surveys on the mainland to provide comprehensive and state-of-the-art radiometric K, eTh and eU grids of the coastal areas of western and central Norway. As the eU concentrations in parts per million (ppm) will correlate with radon concentrations in the near surface of the ground, the uranium compilation from this work forms the foundation of the radon hazard map.

The equivalent uranium (eU) map of the Trøndelag area is based on 12 airborne gamma ray spectrometer surveys that covers a large territory of the county. These measurements reveal a good summary of the ground eU concentration regardless of bedrock or sediment origins.

A supplement to the airborne radiometric surveys is the natural gamma radiation ground measurements, carried out from 1975 to 1992, along all main roads. Based on calibrated scintillometer measurements, bedrock samples were collected, from anomalous sites along the roads, for supplementary XRF analyses. These XRF analytical results reside in the NGU URANAL data base. The ground measurements have the denomination of pulses per. second. The main part of the measured radioactivity is the result of decomposition of uranium, thorium and potassium that exist naturally in the bedrock.

These results can be regarded as a substitute to the airborne radiation measurements, because they identify areas which are likely to be exposed to elevated radon concentrations. They may therefore be useful in areas where we still do not have radiometric data from fixed-wing or helicopter surveys.

The LITO database is another dataset that can be handy to identify sites which are likely to be exposed to elevated radon concentrations. The LITO project was initiated in 1999 and aimed at mapping chemical compositions and petrophysical characteristics of all mapped bedrock units in Norway.

The gathering of samples is based on the national geological maps at a scale of 1:250,000. Each sample is taken from a three metres long core to ensure fresh, un-weathered bedrock. The results are a very comprehensive geochemical and petrophysical national dataset. Based on these LITO samples we have produced map of uranium content by calculating the average values within each geological unit present in the bedrock map of Trøndelag.

This allows us to identify areas which can be exposed to elevated radon concentrations originating from bedrock although Quaternary deposits shield the natural radiation, and also where we do not have airborne uranium measurements.

|  |                                     |                                |
|--|-------------------------------------|--------------------------------|
| <b>Keywords:</b> Geofysikk (Geophysics)          | Radiometri (Radiometrics)           | Tolkning (Interpretation)      |
| Geokjemi (Geochemistry)                          | Radonmåling (Radon detection)       | Uran (Uranium)                 |
| Helikoptermåling (Helicopter-borne measurements) | Flymåling (Fixed-wing measurements) | Fagrapport (Scientific report) |

## CONTENTS

|  |    |
|--|----|
| 1. INTRODUCTION .....  | 7  |
| 2. REGIONAL GEOPHYSICAL MEASUREMENTS OF RADIOACTIVITY FROM<br>AEROPLANE AND HELICOPTER ..... | 9  |
| 2.1 Correction and compilation of airborne radiometric data.....                             | 9  |
| 2.2 Correction and compilation, Trøndelag, Mid Norway .....                                  | 10 |
| 2.3 Reprocessing method .....  | 12 |
| 2.3.1 212 - Grong, Harran - 1988.....  | 12 |
| 2.3.2 270 - Rennebu, Innset .....  | 13 |
| 2.3.3 278 - Steinkjer - 1986.....  | 15 |
| 2.3.4 280 - Andorsjøen, Grong, Snåsavatnet - 1990.....                                       | 15 |
| 2.3.5 281 - Meråker, Flornes - 1991 .....  | 16 |
| 2.3.6 282 - Stiklestad - 1991 .....  | 17 |
| 2.3.7 283 - Verran, Holden, Åfjord - 1992.....   | 17 |
| 2.3.8 289 - Røyrvik - 1993.....  | 18 |
| 2.3.9 289-2 - Skorovatn - 1994.....  | 19 |
| 2.3.10 311 - Vuku - 1992 .....   | 19 |
| 2.4 Calculation of concentrations .....  | 20 |
| 2.5 Grid knitting.....   | 22 |
| 2.6 Uranium map of the Trøndelag area (ppm) .....  | 22 |
| 2.7 Conclusions of grid knitting .....   | 23 |
| 3. CONVERTING THE URANIUM GRID COMPILATION INTO A RADON HAZARD<br>MAP .....                  | 27 |
| 3.1 GAMMA RADIATION GROUND MEASUREMENTS .....  | 35 |
| 3.2 GEOCHEMICAL COMPOSITION OF THE BEDROCK (LITO DATABASE) .....                             | 39 |
| <i>Acknowledgements</i> .....  | 44 |
| 4. REFERENCES.....   | 46 |

## FIGURES

|  |    |
|--|----|
| Figur 1. The map shows the coverage of fixed-wing and helicopter radiometric measurements for the whole country of Norway up to 2018. ....   | 8  |
| Figur 2. Fixed wing and helicopter borne gamma ray spectrometry surveys within the area. Helicopter surveys in red colour. ....  | 9  |
| Figur 3. Survey area map. Each survey has its own colour. ....   | 11 |
| Figur 4. 212 - Grong, Harran - Uranium count, before and after microlevelling. ....  | 13 |
| Figur 5. 270 - Rennebu, Innset - Left: Original uranium cps data. Middle: Multiplication factors (from 0.95 to 1.45) applied to the uranium cps values. Right: Final uranium ppm concentrations. ....  | 14 |
| Figur 6. Linear regression between the uranium ground concentration in the overlapping area of project Trøndelag-2015 (ppm) vs. uranium data (cps) from survey #270. ....  | 14 |
| Figur 7. 278 - Steinkjer - Uranium count, before and after microlevelling. ....  | 15 |
| Figur 8. 280 - Snåsa - Uranium count, before and after microlevelling. ....  | 15 |
| Figur 9. 280 - Snåsavatnet - Uranium count, before and after microlevelling. ....  | 16 |
| Figur 10. 281 - Meråker, Flornes - Uranium count before and after microlevelling. ....   | 16 |
| Figur 11. 282 - Stiklestad - Uranium count, before and after microlevelling. ....  | 17 |
| Figur 12. 283 - Verran, Holden, Åfjord - Uranium count before and after microlevelling. ....   | 18 |
| Figur 13. 289 - Røyrvik - Uranium count, before and after microlevelling. ....   | 19 |
| Figur 14. 289-2 - Skorovatn - Uranium count, before and after microlevelling. ....   | 19 |
| Figur 15. 311 - Vuku - Uranium count, before and after microlevelling. ....  | 20 |
| Figur 16. Example of linear regression used for concentration calculation. ....  | 21 |
| Figur 17. Uranium map of the Trøndelag area (ppm) based on airborne measurements of radiation from both bedrock outcrops and soils. ....   | 23 |
| Figur 18. Uranium grid values originating from bedrock outcrops exclusively. ....  | 25 |
| Figur 19. Uranium grid values originating from Quaternary deposits. ....   | 26 |
| Figur 20. The relationship between annual average indoor radon concentration measurements and eU concentrations in the ground around dwellings in the Oslo area (Smethurst et al., 2017). Red square indicating Trøndelag data spread, is shown in detail in Figure 21. .... | 27 |
| Figur 21. The relationship between annual average indoor radon concentration measurements and eU concentrations in the ground around dwellings in the Trøndelag area. ....   | 28 |
| Figur 22. Dwellings with indoor radon annual average concentrations (Bq/m <sup>3</sup> ). ....   | 29 |
| Figur 23. Oslo region radon potential (% ≥ 200 Bq/m <sup>3</sup> ) and geometric mean of indoor radon concentration as functions of eU concentration in the ground (Smethurst et al., 2017). ....  | 30 |
| Figur 24. Re-scaled enlargement of Figure 23 between 1 and 7 ppm eU (Smethurst et al., 2017). ....   | 30 |
| Figur 25. The graduation of eU (ppm) in three classifications based on fixed-wing and helicopter measurements over the Trøndelag county. ....  | 31 |
| Figur 26. A segment of the classification map from the Grong area. ....  | 32 |
| Figur 27. The segment map in Figure 26 after aggregation (1000 m) and buffering (500 m) of anomaly classification polygons. ....   | 33 |
| Figur 28. Estimated ground concentration of uranium with aggregation distance of 1000 m and buffer distances of 500 m. The graduation of eU (ppm) and radon risk are presented in 4 classifications. ...   | 34 |
| Figur 29. Total gamma radiation, measured with scintillometer along roads in Trøndelag county (Lindahl et al., 1996). ....   | 35 |
| Figur 30. Interpretation map of natural gamma radiation from bedrock. This map may identify areas which are likely to be exposed to elevated radon concentrations (Lindahl et al., 1996). ....   | 36 |
| Figur 31. Distribution of bedrock samples in the URANAL database. ....   | 37 |
| Figur 32. Distribution of XRF analysed bedrock samples from the URANAL database, with uranium content > 10 ppm, within the Trøndelag county. ....  | 38 |
| Figur 33. The distribution of LITO samples up to 2017. ....  | 39 |
| Figur 34. Uranium concentrations in ppm for the LITO samples from Trøndelag. ....  | 40 |
| Figur 35. Average uranium concentrations (ppm) calculated from LITO samples within each bedrock unit. ....   | 41 |
| Figur 36. New national radon risk map – Trøndelag test area. The map is based on both airborne radiometric measurements as well as average geochemical analyses of bedrock samples (LITO project). ....  | 43 |
| Figur 37. Published former radon hazard map based on indoor radon measurements and existing bedrock maps, Trøndelag. ( <a href="http://geo.ngu.no/kart/radon">http://geo.ngu.no/kart/radon</a> ), (Smethurst et al., 2014). ....   | 44 |

## TABLES

|   |    |
|---|----|
| Table 1. Acquisition details, radiometric data, Trøndelag .....                 | 10 |
| Table 2. Survey parameters. Downward-looking detectors are considered only..... | 12 |
| Table 3. 283 - Uranium manual correction. ....                                  | 17 |
| Table 4. Linear regression results. ....  | 21 |
| Table 5. Grid knitting shifts. ....   | 22 |

## 1. INTRODUCTION

The Crustal Onshore-Offshore Project (COOP) was initiated by the Geological Survey of Norway (NGU) in 2010 to study the onshore-offshore relationships along the coast of western Norway. The integrated mapping and research project were originally financed by NGU, Oljedirektoratet (NPD) and the petroleum companies BayernGas (now Spirit Energy), ConocoPhillips, Det norske (now AkerBP), Lundin, Noreco, Statoil (now Equinor), Total and Wintershall (now DEA), with the goal to improve our knowledge of onshore-offshore tectonic links, deep weathering and heat flow along the coast of western Norway. Phase 1 of the project was reported in January 2013 (Olesen et al. 2013), December 2013 (Maystrenko 2013) and June 2014 (Maystrenko 2014). Phase 2 was reported in December 2015 and will be publicly available in December 2020 (Olesen et al. 2015). The energy and petroleum companies BKK, Centrica (now Spirit Energy) DONG (now part of INEOS), Eni (now Vår Energi), E.ON (now part of DEA), GdF Suez (now part of Neptune Energy), Maersk (now part of Total), Repsol, RWE-Dea (now DEA), Statoil (now Equinor), Suncor and VNG (now part of Neptune Energy) joined the project in 2011-2014 as late participants and the project was extended to a Phase 2 including the Møre margin, the Møre-Trøndelag Fault Complex and the Haltenbanken area. The total COOP area includes the Norwegian part of the North Sea and the Mid-Norwegian shelf and the adjacent Norwegian mainland in western and central Norway. The new public roads company, Nye Veier, decided to sponsor the project in 2016. The extra funding from this company financed a new magnetic and radiometric survey in the Agder-Telemark region. COOP Phase 1 and 2 have now a total of 21 external sponsors. Reprocessing of vintage radiometric data and an updated bedrock map from the COOP1 and COOP2 areas are also included. Phase 3 of the project is registered as a separate project at NGU and is financed by Dea, Equinor, Faroe, INEOS, Lundin, Neptune, Petrolia, Repsol, Spirit, Suncor, Total, VNG (now part of Neptune), NPD and NGU. The project will be finished by the end of 2020.

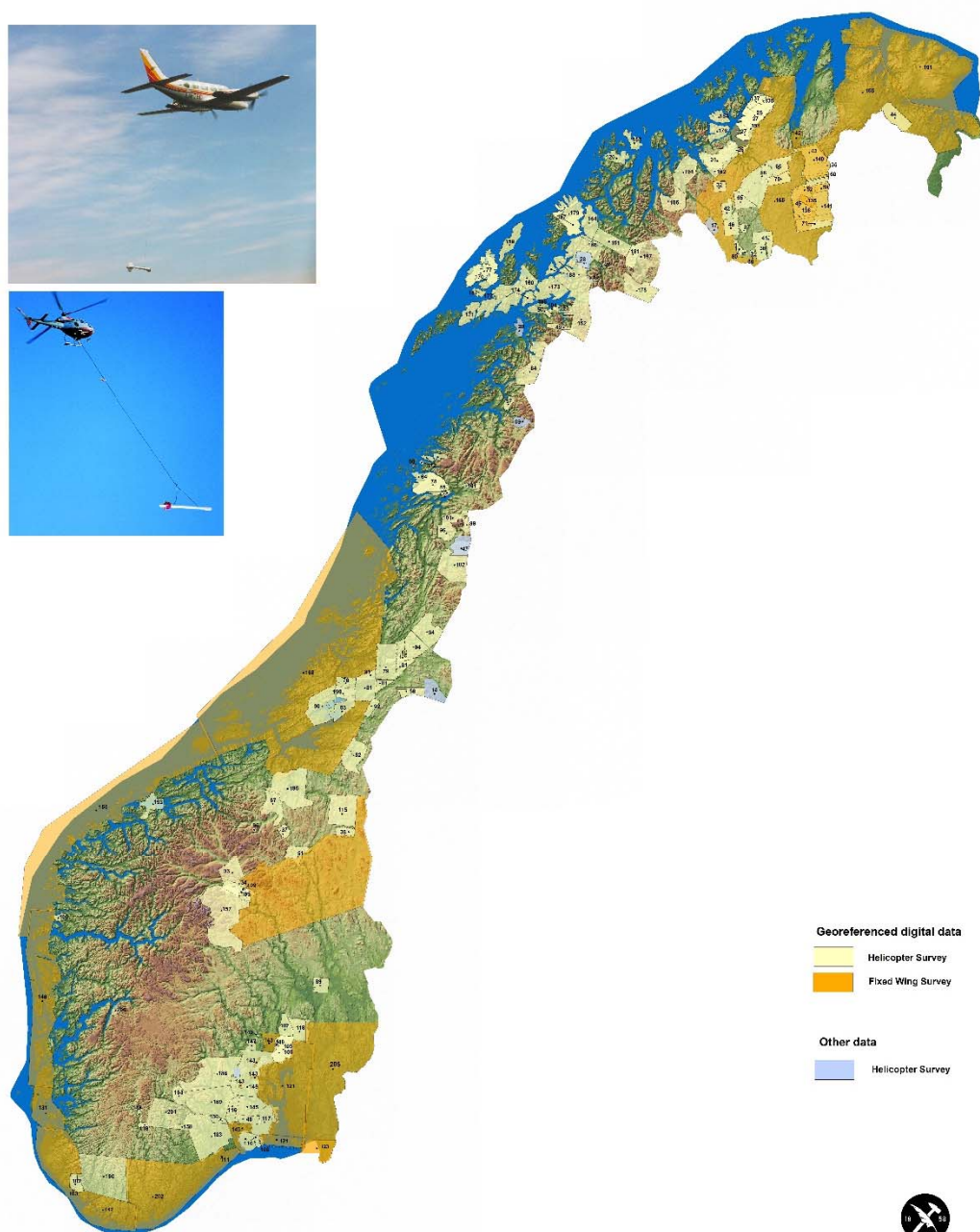
The COOP1 & COOP2 projects include acquisition of five new airborne surveys acquired in the years 2010-2013, in addition to new gravity and heat-flow data. The combined aeromagnetic and radiometric surveys along the coast of western and mid Norway (BESTAS-10, SAS-11, TRAS-13 and AFS-16) have a line spacing of 250 m and a nominal flying altitude of 60 m. NGU has in Phase 2 compiled both new surveys and existing radiometric surveys on the mainland to provide comprehensive and state-of-the-art radiometric K, eTh and eU grids of the coastal areas of western and central Norway. New petrophysical data such as magnetic properties, density and the K, eU and eTh contents from spectrometer measurements on outcrops have been acquired in order to facilitate the interpretation of the new surveys.

The COOP studies have aimed at compiling lithogeochemical information on basement rocks along the coast of western and central Norway with emphasis on characterising the eU, eTh and K contents.

The heat production within the crystalline basement is key to an improved understanding of the varying temperatures in offshore sedimentary basins. The heat production depends on the content of the radioactive elements K, eU and eTh. The petroleum industry has therefore great interest in mapping the content of the radioactive elements along the coast. The eU data can, however, also be used to produce a radon awareness map. The present report documents the compilation of the uranium data and the production of the radon hazard map.

Figure 1 shows radiometric surveys for the whole country of Norway up to 2018. Both fixed-wing and helicopter measurements are represented. These data are of most importance to produce a national radon hazard map.

## Airborne radiometric surveys in Norway



Date: 08.03.2019

  
NORGES  
GEOLOGISKE  
UNDERSØKELSE  
- NGU -

Figur 1. The map shows the coverage of fixed-wing and helicopter radiometric measurements for the whole country of Norway up to 2018.

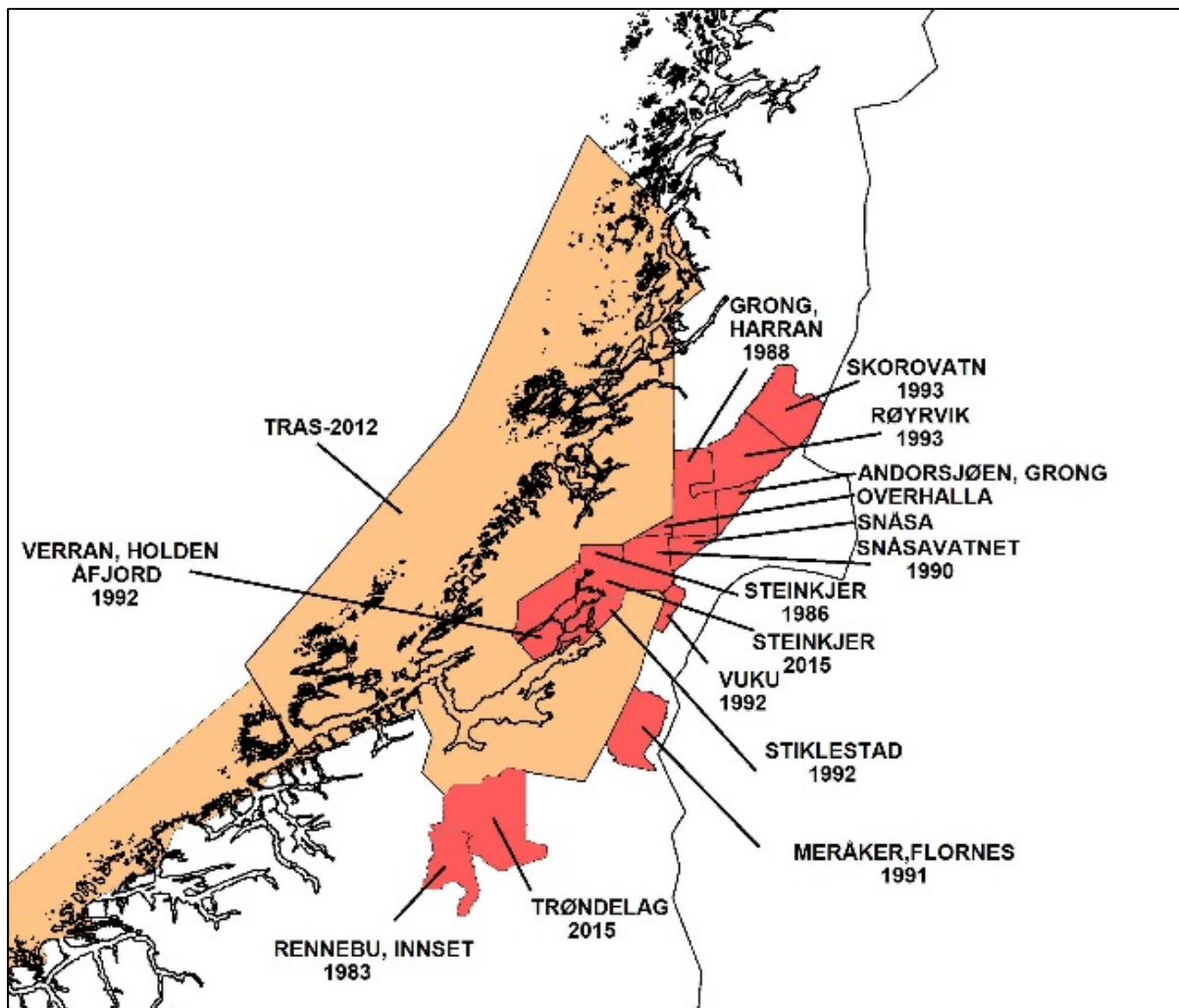
## 2. REGIONAL GEOPHYSICAL MEASUREMENTS OF RADIOACTIVITY FROM AEROPLANE AND HELICOPTER

### 2.1 Correction and compilation of airborne radiometric data

There are many naturally existing radioactive elements. However, only three have isotopes that emit gamma radiation of sufficient intensity to be measured by airborne gamma ray spectrometry. The three major sources of gamma radiation are  $^{40}\text{K}$ , daughter products in the  $^{238}\text{U}$  decay series and daughter products in the  $^{232}\text{Th}$  series.

The multi-channel gamma spectrometry data used in the present study were acquired from fixed-wing and helicopter surveys (1983-2015). Figure 2 shows their locations.

In this project we compiled newly acquired data, such as the surveys TRAS-2012, Steinkjer-2015 and Trøndelag-2015, with previously acquired data in Trøndelag between 1983 and 1993. For these old data, only count rates were available. Thus, concentrations were calculated using the overlap with TRAS-12 survey. Acquisition details are presented in Table 1.



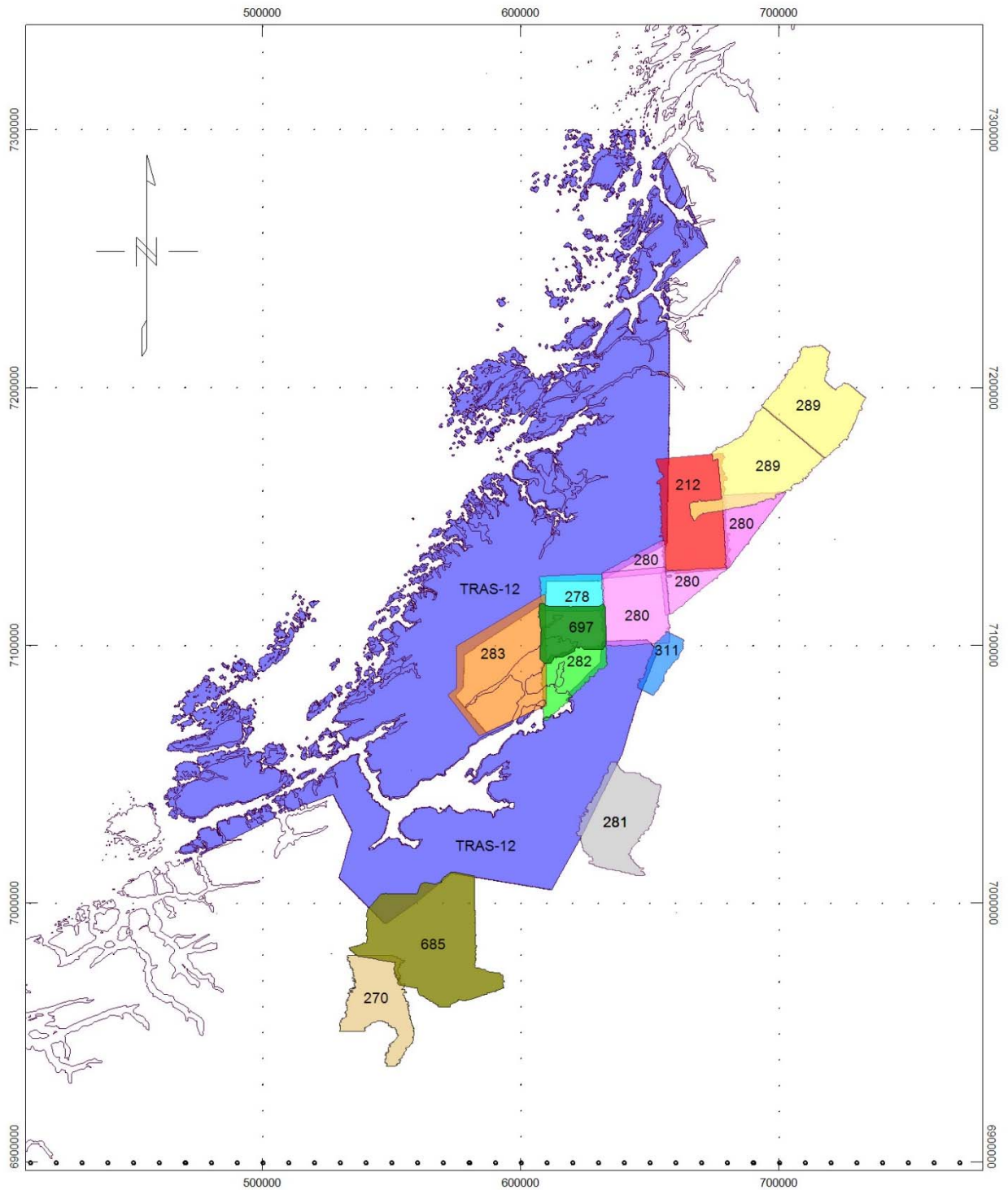
Figur 2. Fixed wing and helicopter borne gamma ray spectrometry surveys within the area. Helicopter surveys in red colour.

Table 1. Acquisition details, radiometric data, Trøndelag.

| DRAGON # / Name | Survey location                                   | Year    | Contractor | Platform   | <i>Flying height (m)</i> | Line spacing (m) | cps/ppm |
|-----------------|---|---------|------------|------------|--------------------------|------------------|---------|
| 212             | Grong, Harran                                     | 1988    | NGU        | Helicopter | 60                       | 250              | cps     |
| 270             | Rennebu, Innset                                   | 1983    | NGU        | Helicopter | 60                       | 200              | cps     |
| 278             | Steinkjer   | 1986    | NGU        | Helicopter | 60                       | 200              | cps     |
| 280             | Andorsjøen, Grong, Snåsavatnet (Snåsa, Overhalla) | 1990    | NGU        | Helicopter | 60                       | 200              | cps     |
| 281             | Meråker, Flornes                                  | 1991    | NGU        | Helicopter | 60                       | 200              | cps     |
| 282             | Stiklestad  | 1991    | NGU        | Helicopter | 60                       | 200              | cps     |
| 283             | Verran, Holden, Åfjord                            | 1992    | NGU        | Helicopter | 60                       | 200              | cps     |
| 289             | Røyrvik, Skorovatn                                | 1993/94 | NGU        | Helicopter | 60                       | 100/200          | cps     |
| 311             | Vuku  | 1992    | NGU        | Helicopter | 60                       | 100              | cps     |
| 00335           | Trøndelag Region Airborne Survey (TRAS)           | 2012-14 | Novatem    | Fixed-wing | 60                       | 250              | ppm     |
| 685             | Trøndelag   | 2015    | NGU        | Helicopter | 83                       | 200              | ppm     |
| 697             | Steinkjer   | 2015    | NGU        | Helicopter | 90                       | 250              | ppm     |

## 2.2 Correction and compilation, Trøndelag, Mid Norway

All the projects of interest for this compilation are listed in Table 1, with their reference number from NGU's DRAGON database, location and year of acquisition. They are also presented in the map below (Figure 3). All data were previously processed and assumed corrected for dead-time, stripping ratio, attenuation, background and standard temperature and pressure (STP) height corrections (IAEA 1991). For all these projects, only the count rates were available. Between June 2012 and March 2014, Novatem, a Canadian airborne geophysics company, carried out an airborne geophysics survey in the Trøndelag region (Trøndelag Region Airborne Survey (TRAS-12) for NGU (Novatem 2014). The uranium data are presented in this section.



Figur 3. Survey area map. Each survey has its own colour.

All these surveys are helicopter-borne using NGU equipment except TRAS-12 which was acquired by an external company *Novatem* with an aircraft equipped with similar equipment.

All these projects have been acquired with various survey parameters as listed below, Table 2.

Table 2. Survey parameters. Downward-looking detectors are considered only.

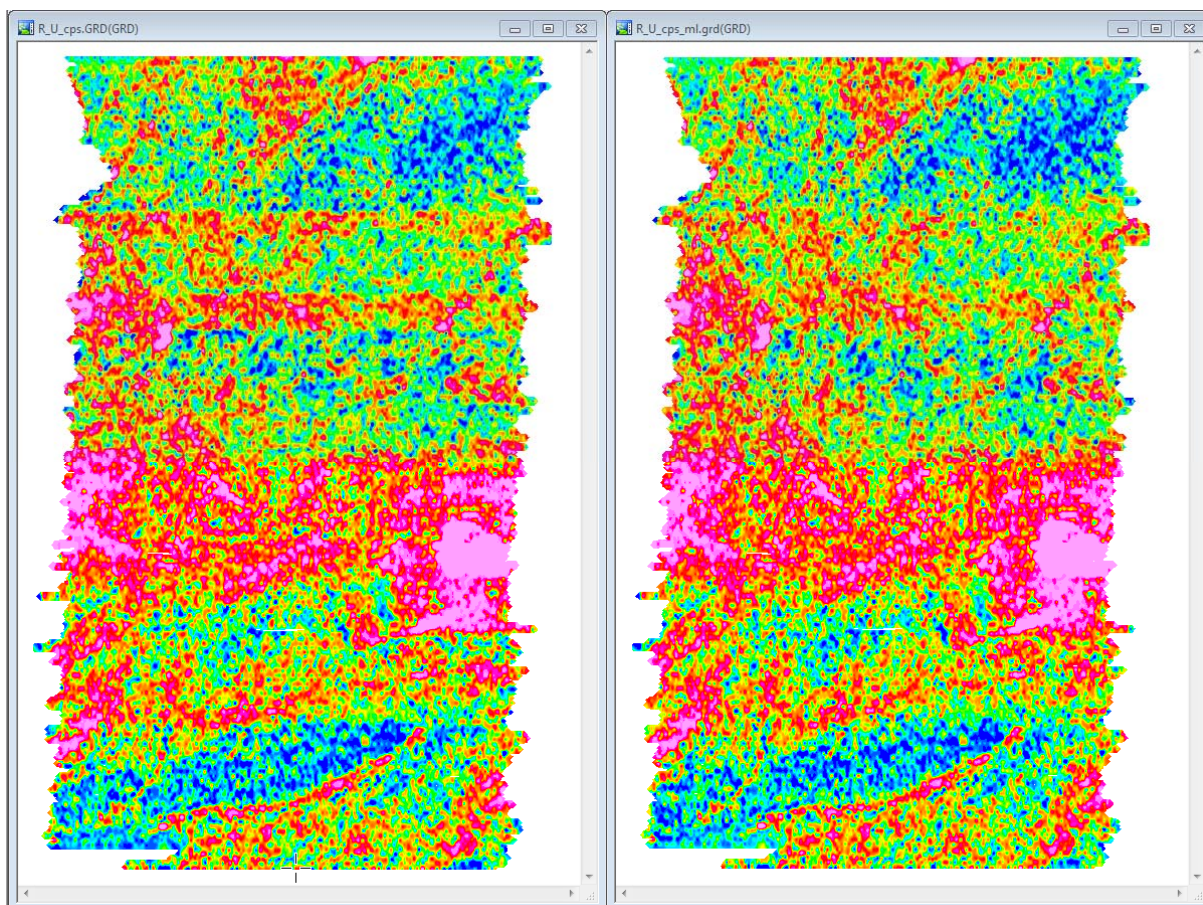
| DRAGON #<br>/ Name | Aircraft   | Altitude<br>(m) | Radiometric instrument                                  | # crystals | Volume<br>(L) |
|--------------------|--|-----------------|---|------------|---------------|
| 212                | Helicopter -<br><i>Aerospatiale Ecureuil<br/>SA 350 B1</i> | 60              | <i>Geometrics GR-800</i>                                | 4          | 16.8          |
| 270                | Helicopter -<br><i>Aerospatiale Ecureuil<br/>SA 350 B1</i> | 60              | <i>Geometrics GR-800</i>                                | 4          | 16.8          |
| 278                | Helicopter -<br><i>Aerospatiale Ecureuil<br/>SA 350 B1</i> | 60              | <i>Geometrics GR-800</i>                                | 4          | 16.8          |
| 280                | Helicopter -<br><i>Aerospatiale Ecureuil<br/>SA 350 B1</i> | 60              | <i>Geometrics GR-800</i>                                | 4          | 16.8          |
| 281                | Helicopter -<br><i>Aerospatiale Ecureuil<br/>SA 350 B1</i> | 60              | <i>Geometrics GR-800</i>                                | 4          | 16.8          |
| 282                | Helicopter -<br><i>Aerospatiale Ecureuil<br/>SA 350 B1</i> | 60              | <i>Geometrics GR-800</i>                                | 4          | 16.8          |
| 283                | Helicopter -<br><i>Aerospatiale Ecureuil<br/>SA 350 B1</i> | 60              | <i>Geometrics GR-800</i>                                | 4          | 16.8          |
| 289                | Helicopter -<br><i>Aerospatiale Ecureuil<br/>SA 350 B1</i> | 60              | <i>Geometrics GR-800 /<br/>Exploranium GR820 (1994)</i> | 4          | 16.8          |
| 311                | Helicopter -<br><i>Aerospatiale Ecureuil<br/>SA 350 B1</i> | 60              | <i>Geometrics GR-800</i>                                | 4          | 16.8          |
| 00335              | Piper Navajo PA-31   | 60              | <i>Radiation Solutions RSX-5</i>                        | 8          | 33.4          |
| 685                | Helicopter -<br><i>Aerospatiale Ecureuil<br/>SA 350 B2</i> | 60              | <i>Radiation Solutions RSX-5</i>                        | 4          | 16.8          |
| 697                | Helicopter -<br><i>Aerospatiale Ecureuil<br/>SA 350 B2</i> | 60              | <i>Radiation Solutions RSX-5</i>                        | 4          | 16.8          |

## 2.3 Reprocessing method

Several datasets, mainly uranium counts, needed to be reprocessed prior to concentration calculation and merging. The filtering and editing required is described below.

### 2.3.1 212 - Grong, Harran - 1988

The original uranium data displayed a horizontal noise trend near the top of the grid (Rønning, 1990). Hence, a microlevelling was required to enhance the data. A decorrugation cutoff wavelength of 4000 m and a Naudy filter of 500 m were used (Figure 4).



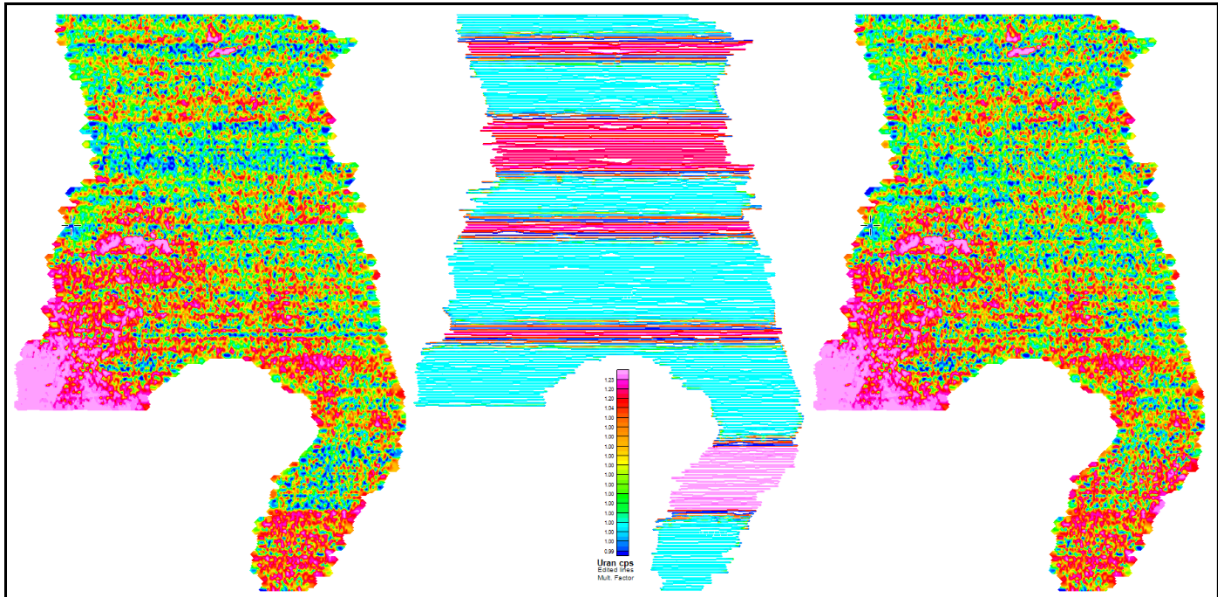
Figur 4. 212 - Grong, Harran - Uranium count, before and after microlevelling

### 2.3.2 270 - Rennebu, Innset

For data analysis and comparison, the count rates (Håbrekke 1983) must be converted to the relevant ground concentrations. In this case, the data are 35 years old with very little information of their acquisition. To calculate the ground concentrations from these data, a reference must be used. The dataset overlapped with Trøndelag-2015 survey area. For the overlap area, points are plotted in a graph from which the linear regression is calculated.

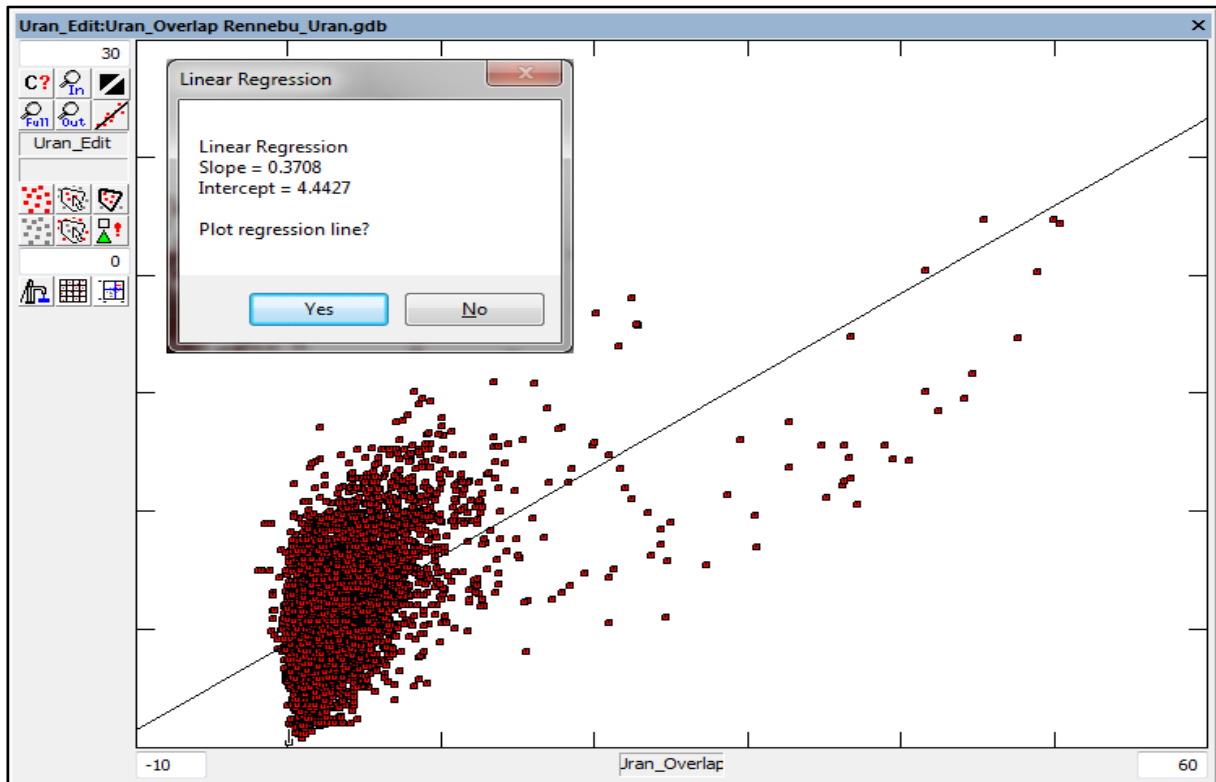
A manual process of adjusting the uranium count-rates from lines with relative higher or lower count rates were performed. Some lines had a visible deviation in the uranium count rate, compared to their adjacent lines, mostly due to variations in temperature, ground and air moisture, radon level and flying height, thus making it necessary to perform a manual levelling of some areas.

The aim of this adjustment process was to produce a uniform grid, while matching the calculated Rennebu-Innset uranium concentrations with the recent data from Trøndelag-2015, which was processed according to IAEA standards, with all normal corrections applied, with the relatively large overlapping area used as a reference.



Figur 5. 270 - Rennebu, Innset - Left: Original uranium cps data. Middle: Multiplication factors (from 0.95 to 1.45) applied to the uranium cps values. Right: Final uranium ppm concentrations.

This provided a good control for levelling, but as most of the overlap is in a low uranium concentration area, the majority data points are in the lower end of the cps scale, where the Geometrics GR-820 spectrometer instrument is less sensitive and thus less accurate.

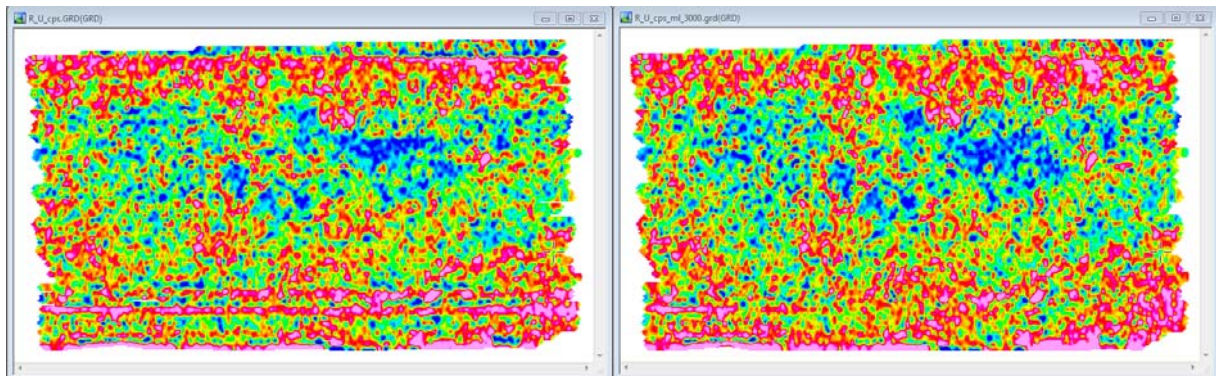


Figur 6. Linear regression between the uranium ground concentration in the overlapping area of project Trøndelag-2015 (ppm) vs. uranium data (cps) from survey #270.

A final uranium concentration value for the Rennebu-Innset area was calculated using a count-per-second cutoff value of 4, and a slope of 0.35 ppm/cps. This was the result of a thorough iterative process, which produced the best fitting concentration values for the overlap area. This made it possible to use the grid knitting procedure in Geosoft Oasis Montaj to produce a seamless grid for the whole area.

### 2.3.3 278 - Steinkjer - 1986

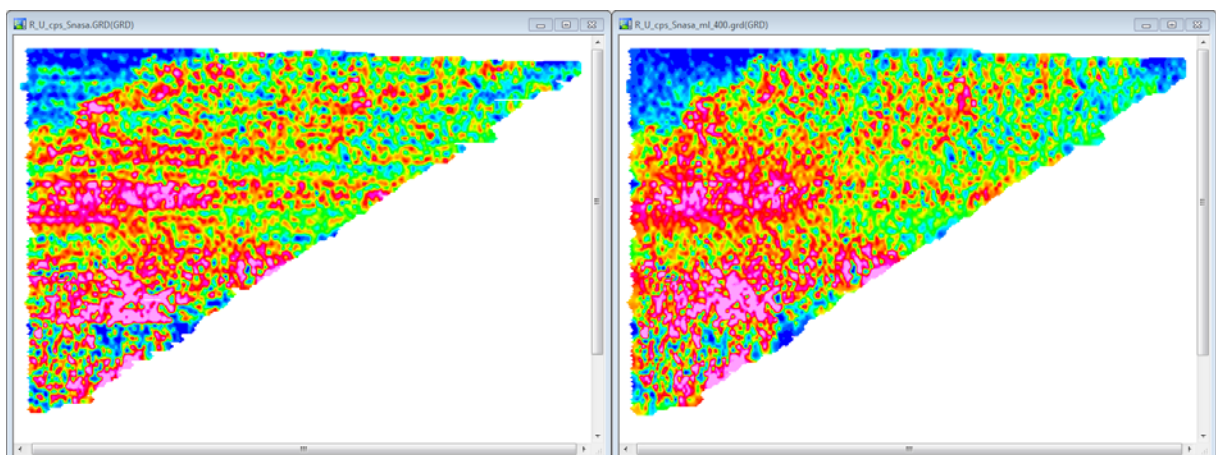
The original uranium data displayed horizontal noise trends at the bottom of the grid (Mogaard, 1989). A microlevelling was required to enhance the data. A decorrugation cutoff wavelength of 3000 m and a Naudy filter of 400 m were used (Figure 7).



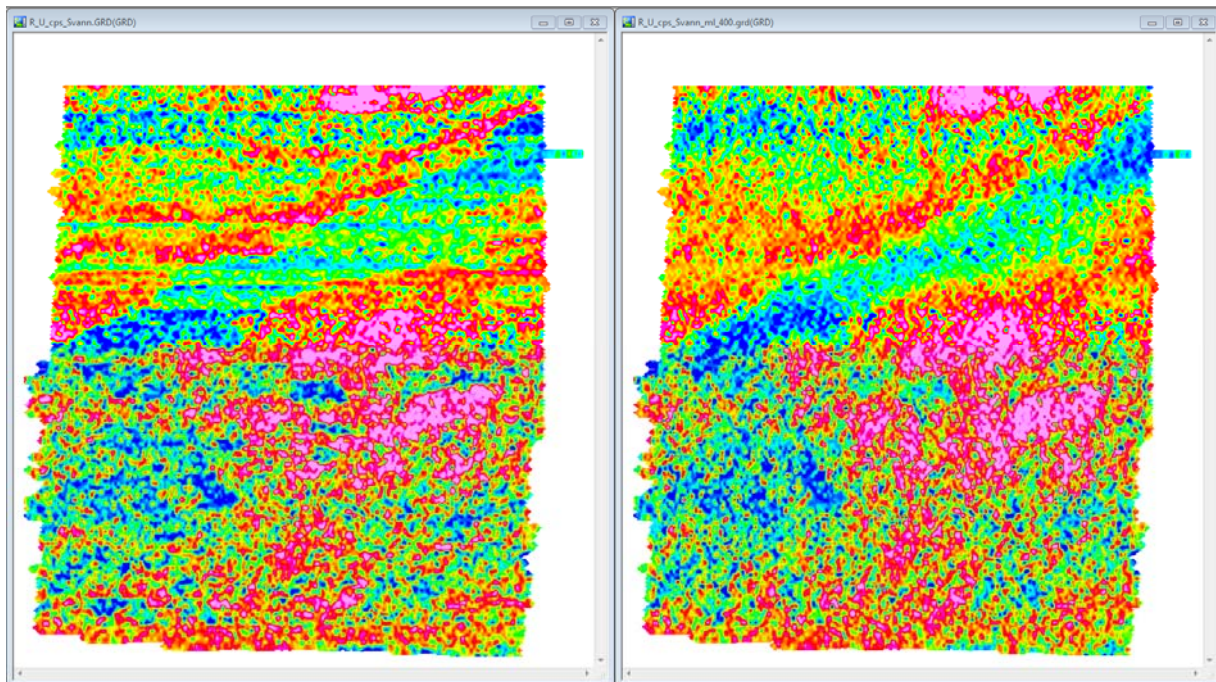
Figur 7. 278 - Steinkjer - Uranium count, before and after microlevelling.

### 2.3.4 280 - Andorsjøen, Grong, Snåsavatnet - 1990

This area consists of four sub-areas: Andorsjøen, Snåsa, Snåsavatnet and Overhalla (Rønning, 1991; 1992a; 1992b & 1992c). Of these four datasets, only the Snåsa and Snåsavatnet uranium grids displayed noisy trends. For both grids, a light microlevelling was applied to enhance the quality of the data, with a decorrugation cutoff wavelength of 3000 m and a Naudy filter of 400 m (Figure 8 and Figure 9).



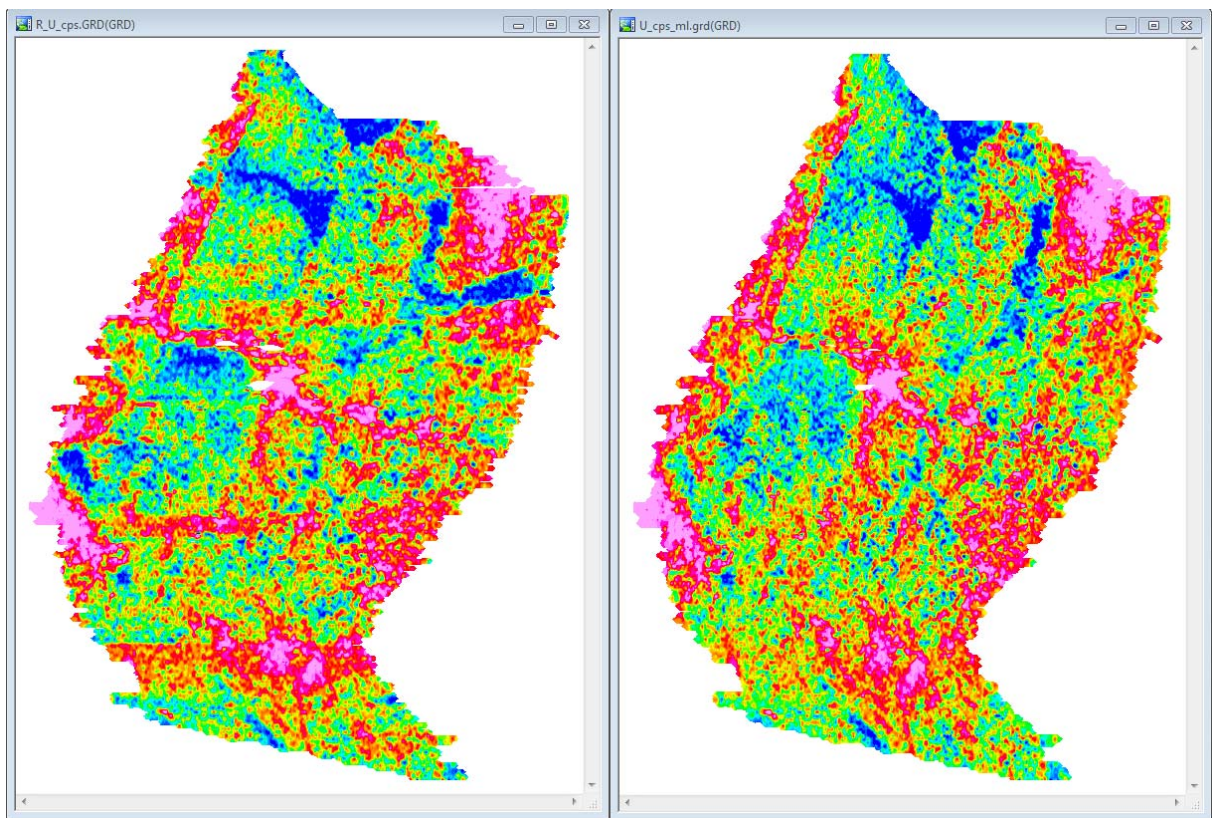
Figur 8. 280 - Snåsa - Uranium count, before and after microlevelling.



Figur 9. 280 - Snåsavatnet - Uranium count, before and after microlevelling.

### 2.3.5 281 - Meråker, Flornes - 1991

The original uranium data displayed several horizontal noise trends (Mogaard, 1993). A microlevelling was required to enhance the cutoff wavelength of 8000 m and a Naudy filter of 1000 m were used (Figure 10).

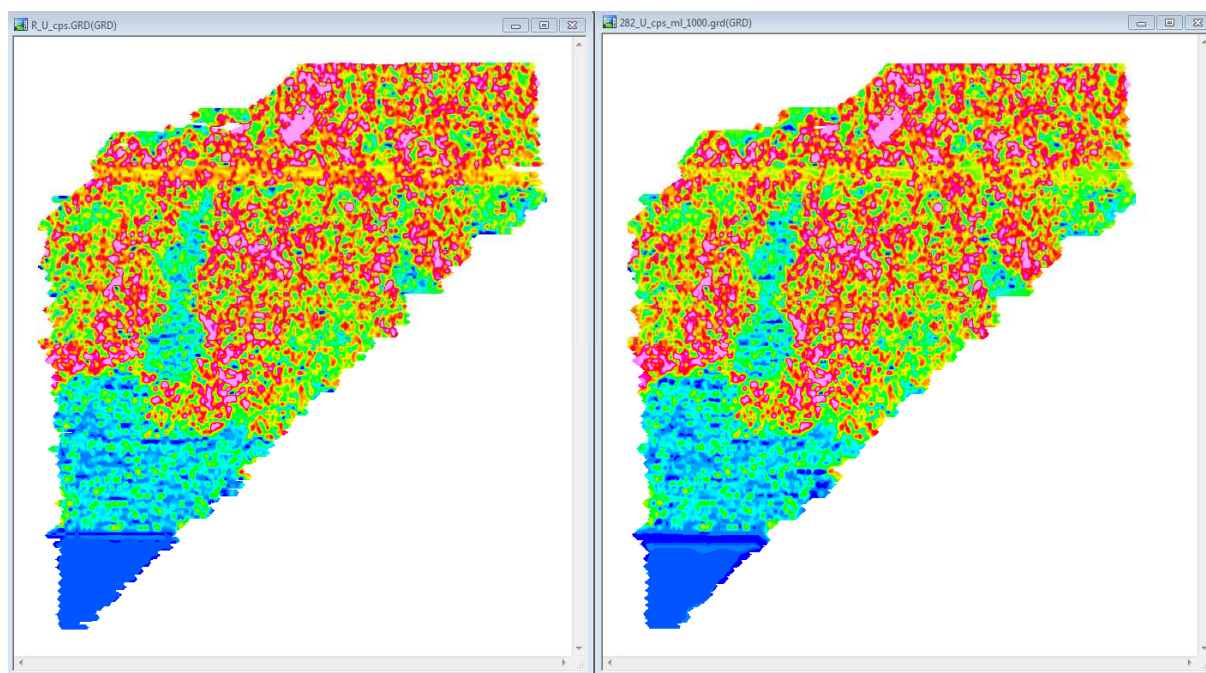


Figur 10. 281 - Meråker, Flornes - Uranium count before and after microlevelling.

### 2.3.6 282 - Stiklestad - 1991

The original uranium data displayed a horizontal noise trend near the top of the grid (Rønning, 1995a). A microlevelling was required to enhance the data. A decorrugation cutoff wavelength of 4000 m and a Naudy filter of 1000 m were used (Figure 11).

There is also a stripe at the bottom of the grid. Since this part of the data is above water and disregarded during the merging process, no action was taken to minimize this noise.



Figur 11. 282 - Stiklestad - Uranium count, before and after microlevelling.

### 2.3.7 283 - Verran, Holden, Åfjord - 1992

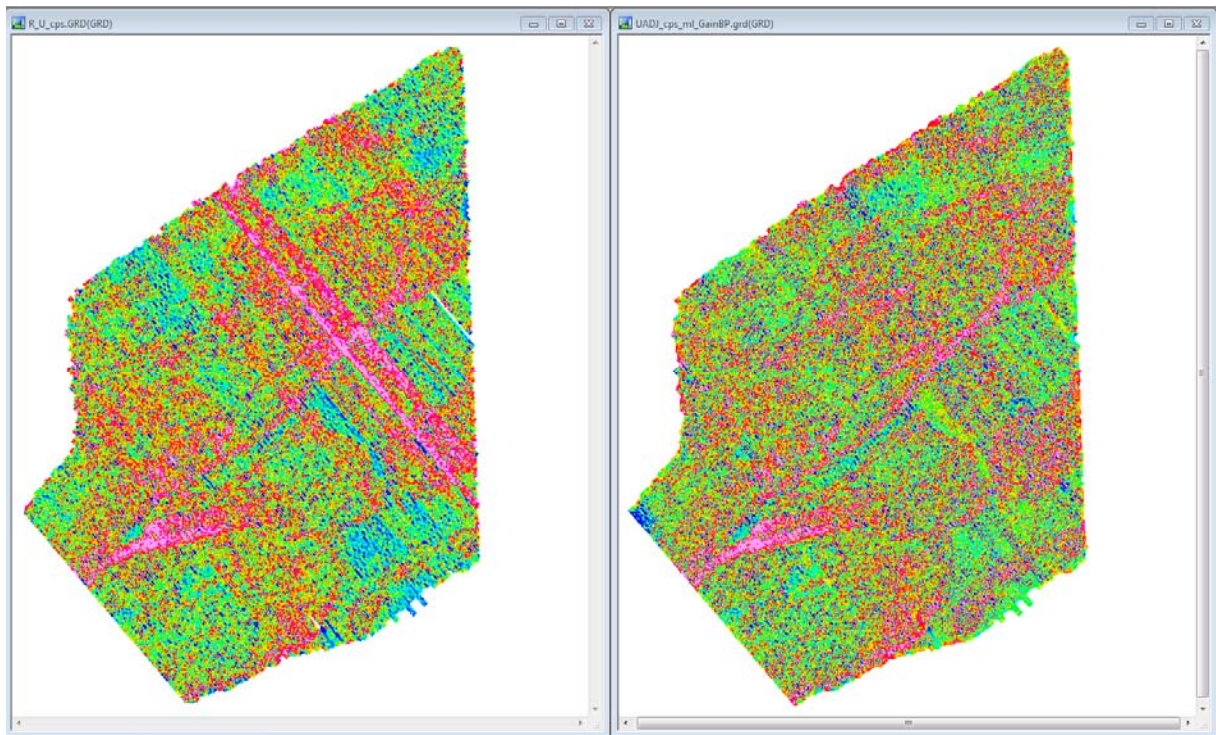
This dataset was flown in 1992 above several water bodies (Rønning, 1995c).

The original uranium data displayed a linear noise trend along the lines. In this dataset, the noise level in some areas is as high as the uranium signature itself. It is also noted that the background on land and on water is very similar. To reflect a consistent background and improve the levelling, lines were initially manually levelled (Table 3).

Table 3. 283 - Uranium manual correction.

| Line       | Uranium adjustment (cps) |
|------------|--------------------------|
| 670        | -12                      |
| 680        |                          |
| 690        |                          |
| 750        | -8                       |
| 760        |                          |
| 770        |                          |
| 780        |                          |
| 790        |                          |
| 791        |                          |
| All others | 0                        |

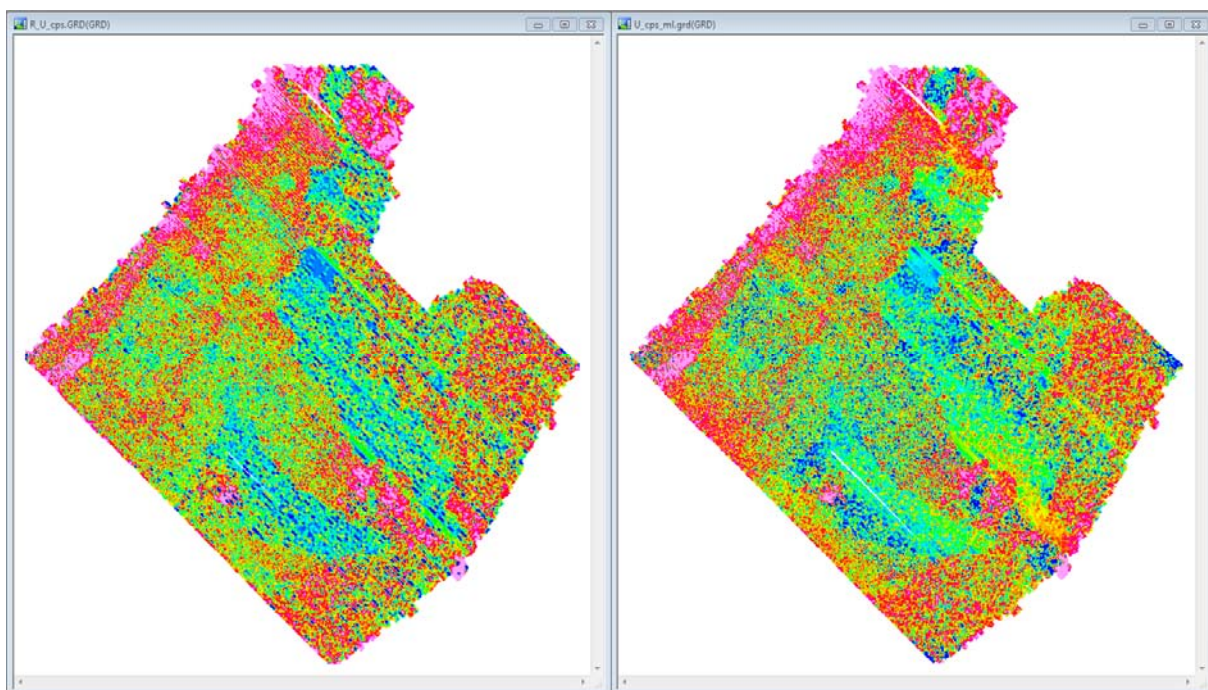
Following the coarse adjustment, a microlevelling was applied to the data, a decorrugation cutoff wavelength of 10,000 m and a Naudy filter of 1000 m (Figure 12).



*Figur 12. 283 - Verran, Holden, Åfjord - Uranium count before and after microlevelling.*

### 2.3.8 289 - Røyrvik - 1993

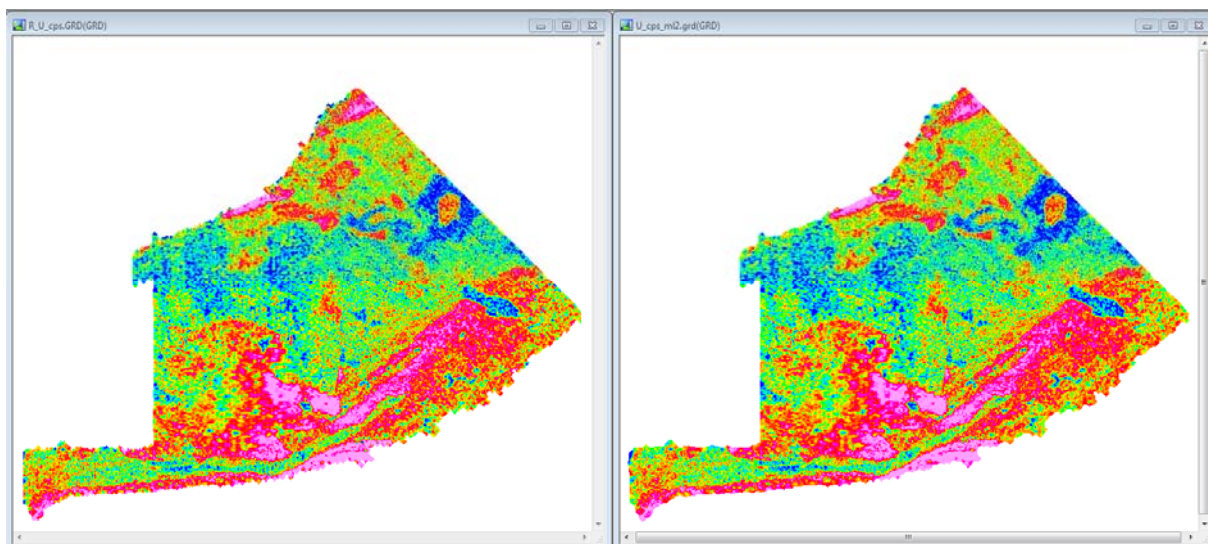
The Røyrvik, Skorovatn areas were flown over two summer seasons. A slight misfit appears between several lines for the uranium element count grids (Rønning, 1995b). A microlevelling was performed on the uranium grid to enhance the final data. A decorrugation cutoff wavelength of 10,000 m and a Naudy filter of 1000 m were used (Figure 13).



Figur 13. 289 - Røyrvik - Uranium count, before and after microlevelling.

### 2.3.9 289-2 - Skorovatn - 1994

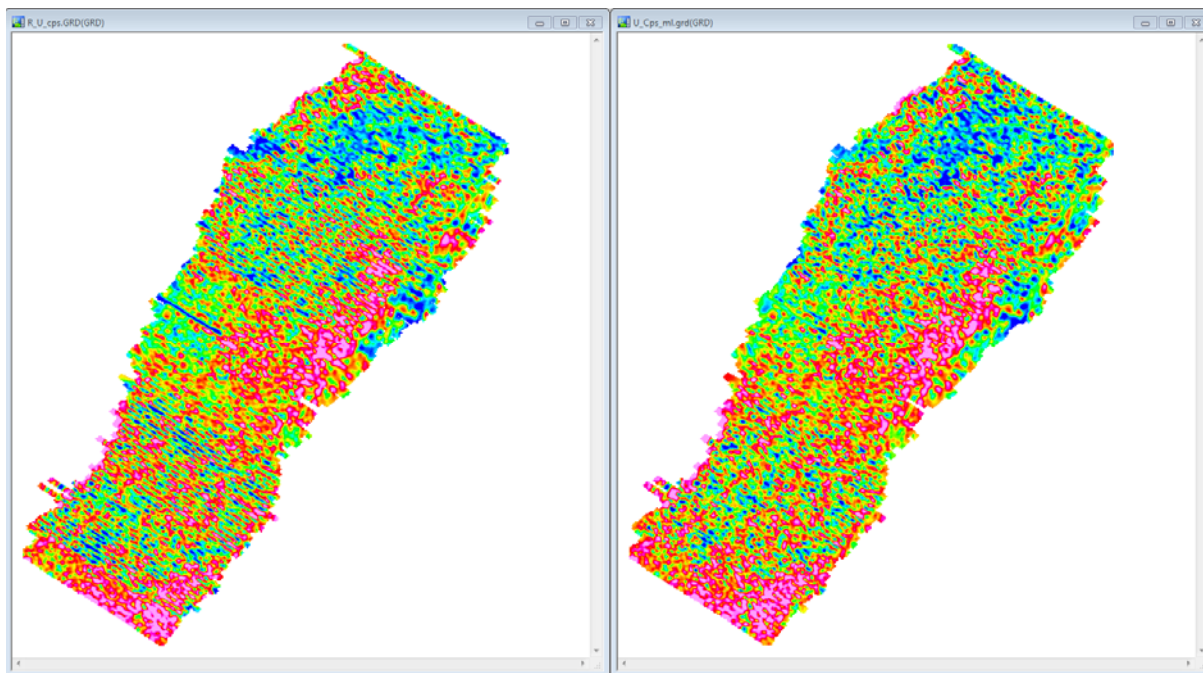
This dataset shows faint stripes in the northernmost corner and at the southwestern tip of the uranium grid (Rønning, 1995b). This area was flown in two line directions of 0° and 135°. Two microlevelling processes with a decorrugation cutoff wavelength of 400 m and a Naudy filter of 500 m were applied to the data for each line direction (Figure 14).



Figur 14. 289-2 - Skorovatn - Uranium count, before and after microlevelling.

### 2.3.10 311 - Vuku - 1992

Faint linear noisy trends are seen on the uranium count grid for the Vuku area (Skilbrei, 1993). A microlevelling was performed on the uranium grid to enhance the final data. A decorrugation cutoff wavelength of 9,000 m, a Naudy filter of 500 m were used (Figure 15).



Figur 15. 311 - Vuku - Uranium count, before and after microlevelling.

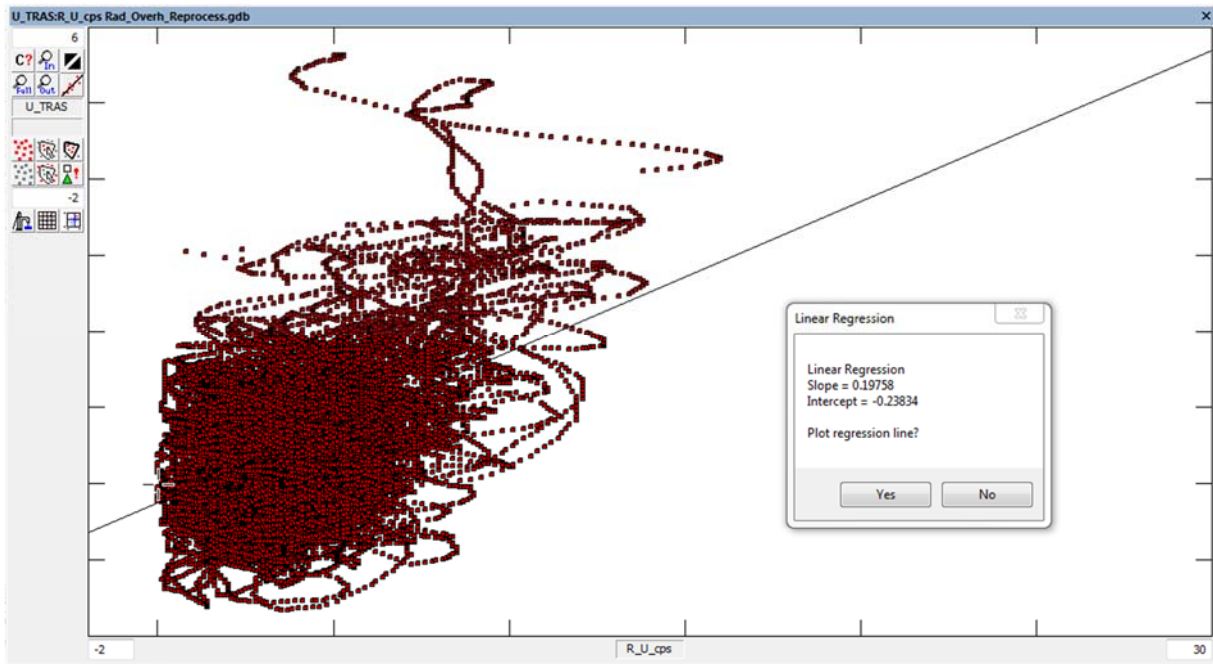
## 2.4 Calculation of concentrations

For data analysis and comparison, the count rates were adjusted to the relevant ground concentrations. Normally, the ground concentrations of the radio-elements are calculated using the so-called sensitivity coefficients obtained from a calibration test (IAEA 1991). By using a calibrated portable spectrometer and recording airborne data of few passes on one and the same line, the sensitivity coefficients are measured.

$$C_e = \frac{n_e}{S_e}$$

The *concentration*  $C$  of a given *element*  $e$  (Th, K or U) is proportional to the *sensitivity coefficient*  $S$  and to the *count rate*  $n$  corrected for dead-time, stripping ratio, background and attenuation.

In this case, data are sometimes 30 years old with very little information on their acquisition. To obtain the concentrations from these data, a concentration reference must be used. As most datasets overlapped with TRAS-12 radiometric grids, they were used as a reference to calculate the concentration. As seen above, a linear correlation exists between the count values and the concentration values. For the overlap area, all points are plotted in a graph from which the linear regression is calculated.



Figur 16. Example of linear regression used for concentration calculation.

The Figure 2.16 shows an example of a linear regression in an overlapped area between projects TRAS-12 (Concentration) and survey #280 (Counts per second). In this case, the uranium linear regression is calculated. The slope and intercept calculated by the Geosoft module are later used for the concentration estimation of survey #280:

$$C_{280} = an_{280} + b$$

In this example, C is the concentration for the uranium data of survey #280, n is the count rate for the uranium data of survey #280 and a and b are the slope and intercept, respectively, as calculated from the linear regression.

The slope and intercept, for each grid, are shown in Table 4:

Table 4. Linear regression results.

| Project | Element | Slope    | Intercept |
|---------|---------|----------|-----------|
| 212     | U       | 0.13862  | -0.54648  |
| 270     | U       | 0.3708   | 4.4427    |
| 278     | U       | 0.018252 | 1.2436    |
| 280     | U       | 0.19758  | -0.23834  |
| 281     | U       | 0.082348 | -0.29926  |
| 282     | U       | 0.10181  | 0.82783   |
| 283     | U       | 0.020547 | 1.0229    |
| 289     | U       | 0.0229   | 1.0061    |
| 311     | U       | 0.04473  | 0.53630   |

The calculation of uranium concentration proved to be a problem for several of the datasets. The count rate level was often within the noise of the instrument. The very low values of the concentration level calculated in TRAS-12 and the low level of the count rates of NGU surveys made the regression calculation uncertain. Several attempts were made, and the best fitted grid was produced using the coefficient from survey #280.

## 2.5 Grid knitting

Grids are merged together using the Geosoft Oasis Montaj tool called Grid Knitting. In the process, a slight shift is introduced to match the grids. Shifts have been calculated as:

$$Shift = E_{comp} - E_{XXX},$$

E is the element grid (uranium in our case), comp the compilation and XXX the project number

The average shift within any one grid is recorded in Table 5.

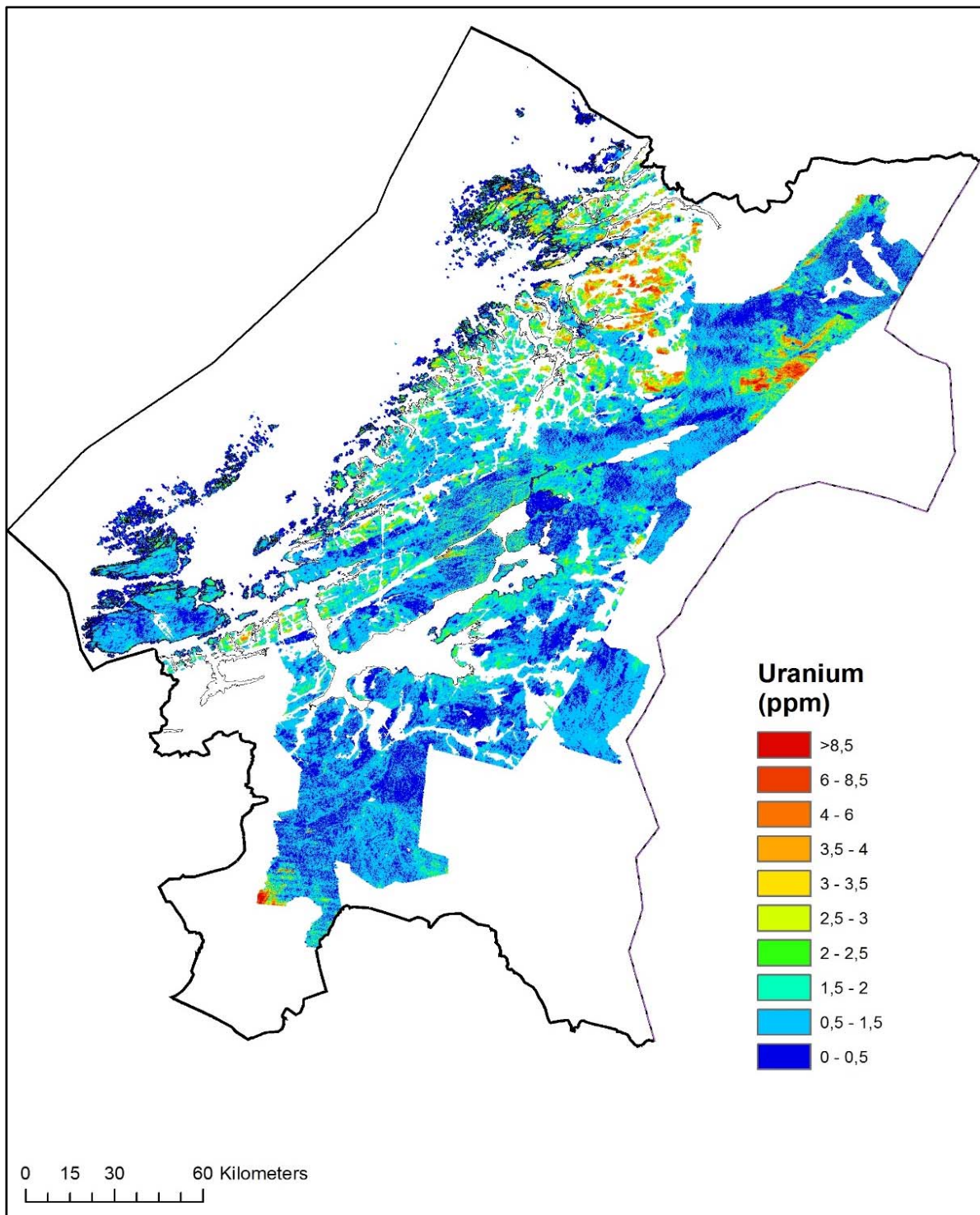
Table 5. Grid knitting shifts.

| Project Code | Project Name   | Year    | Shift Uranium (ppm) |
|--------------|--|---------|---------------------|
| 212          | Grong, Harran  | 1988    | -0.02               |
| 270          | Rennebu, Innset  | 1983    | neglectable         |
| 278          | Steinkjer  | 1986    | 0.03                |
| 280          | Andorsjøen Grong<br>Snåsavatnet<br>Snåsa,<br>Overhalla | 1990    | 0.02                |
|              |  |         | 0.01                |
|              |  |         | 0.01                |
|              |  |         | -0.01               |
| 281          | Meråker, Flornes                                       | 1991    | neglectable         |
| 282          | Stiklestad   | 1991    | 0.11                |
| 283          | Verran, Holden,<br>Åfjord                              | 1992    | neglectable         |
| 289          | Røyrvik, Skorovatn                                     | 1993/94 | neglectable         |
|              |  |         | -0.06               |
| 311          | Vuku   | 1992    | neglectable         |
| 00335        | Trøndelag Region<br>Airborne Survey<br>(TRAS)          | 2012-14 | 0.00                |
| 697          | Steinkjer  | 2015    | neglectable         |
| 685          | Trøndelag  | 2015    | neglectable         |

The shifts of the various grids after the knitting process are much lower than the resolution of the data itself. The final grid is also very consistent.

## 2.6 Uranium map of the Trøndelag area (ppm)

The uranium grids were compiled with a grid cell size of 50x50 m. The map is presented below (Figure 17).



*Figur 17. Uranium map of the Trøndelag area (ppm) based on airborne measurements of radiation from both bedrock outcrops and soils.*

## 2.7 Conclusions of grid knitting

We were able to improve the quality of all uranium datasets flown between 1983 and 1994 by manual adjustments and microlevelling techniques. The main difficulty was the very low counts per second. The reprocessed grids were very consistent from one to another and the merging step did not create any

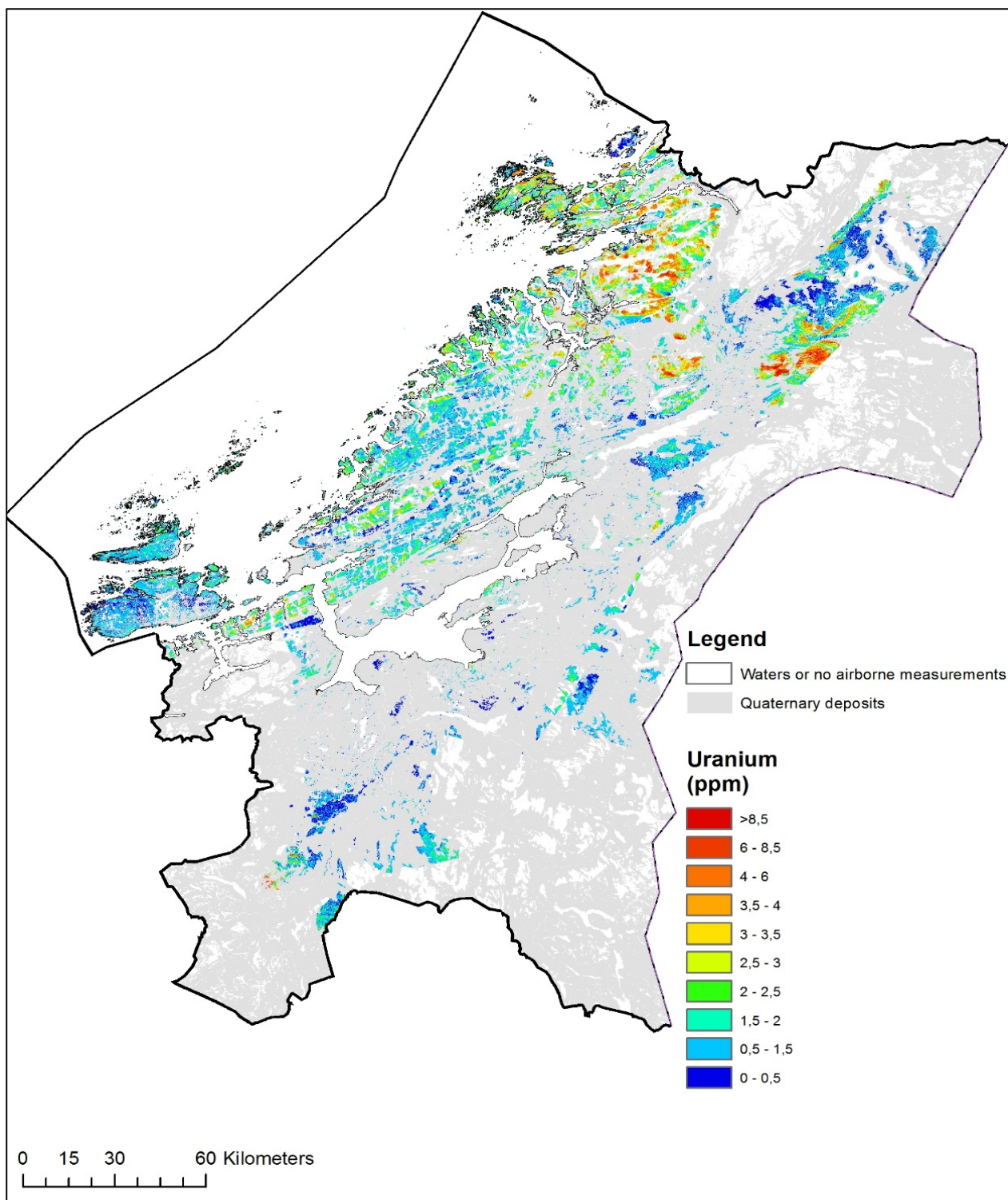
major artefacts. The resulting map (eU) is available in UTM zone 32N projection at WGS-84 datum. The uranium data from each survey were gridded with a grid cell size of 50 x 50 meters. The surveys were then compiled. The result of this combination is presented in Figure 17.

The flight altitude above ground level is an important operational variable, because gamma rays are attenuated by air, and corrections must be made for variations in flight altitude. As a general rule spectrometric data obtained at an altitude greater than 250 m will be of little value. Thus, data from a flight altitude greater than 250 m have been masked.

One should also keep in mind that the uranium grid map is based on radiation from both bedrock outcrops and Quaternary deposits. Thus, some Quaternary deposits consist of radioactive material while other covering deposits, like clays, will shield natural radiation from bedrock.

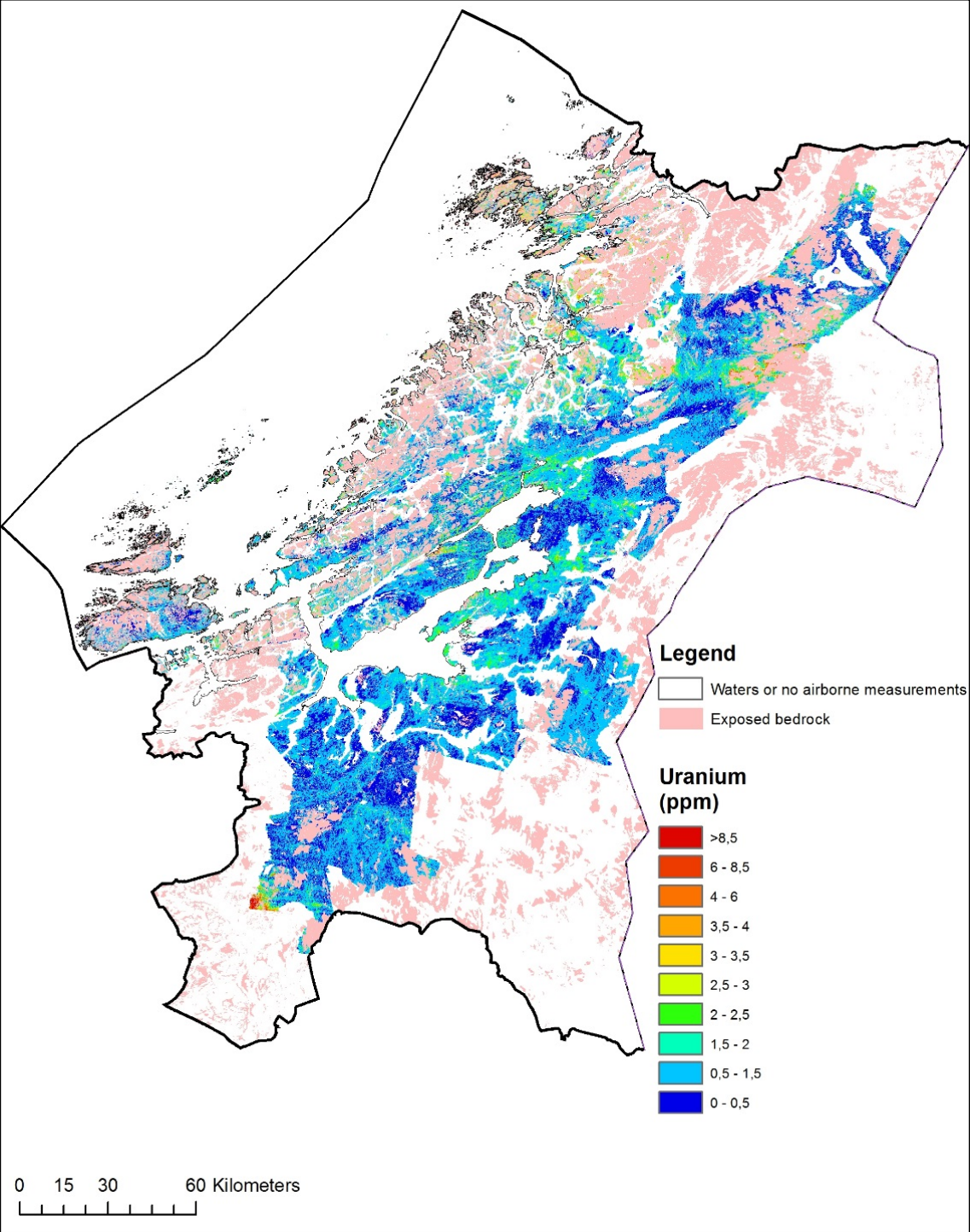
It is nevertheless possible to distinguish radiation from the Quaternary deposits and bedrock outcrops. The precision of such a presentation is certainly dependent on the resolution of the Quaternary deposit map.

By combining the uranium grid values from the airborne measurements (Figure 17) with the Quaternary deposits map, we can display uranium grid values originating from bedrock outcrops exclusively (Figure 18). Gray colored areas in the figure indicate Quaternary deposits. White colored areas represent either water surfaces, which also shield natural radiation, or bedrock outcrops with no airborne measurements.



Figur 18. Uranium grid values originating from bedrock outcrops exclusively.

In the same way we can show a map indicating uranium grid values originating from merely Quaternary deposits (Figure 19). Pink colored areas in the figure indicate bedrock outcrops. White colored areas represent either water surfaces, which also shield natural radiation, or areas with no airborne measurements.



Figur 19. Uranium grid values originating from Quaternary deposits

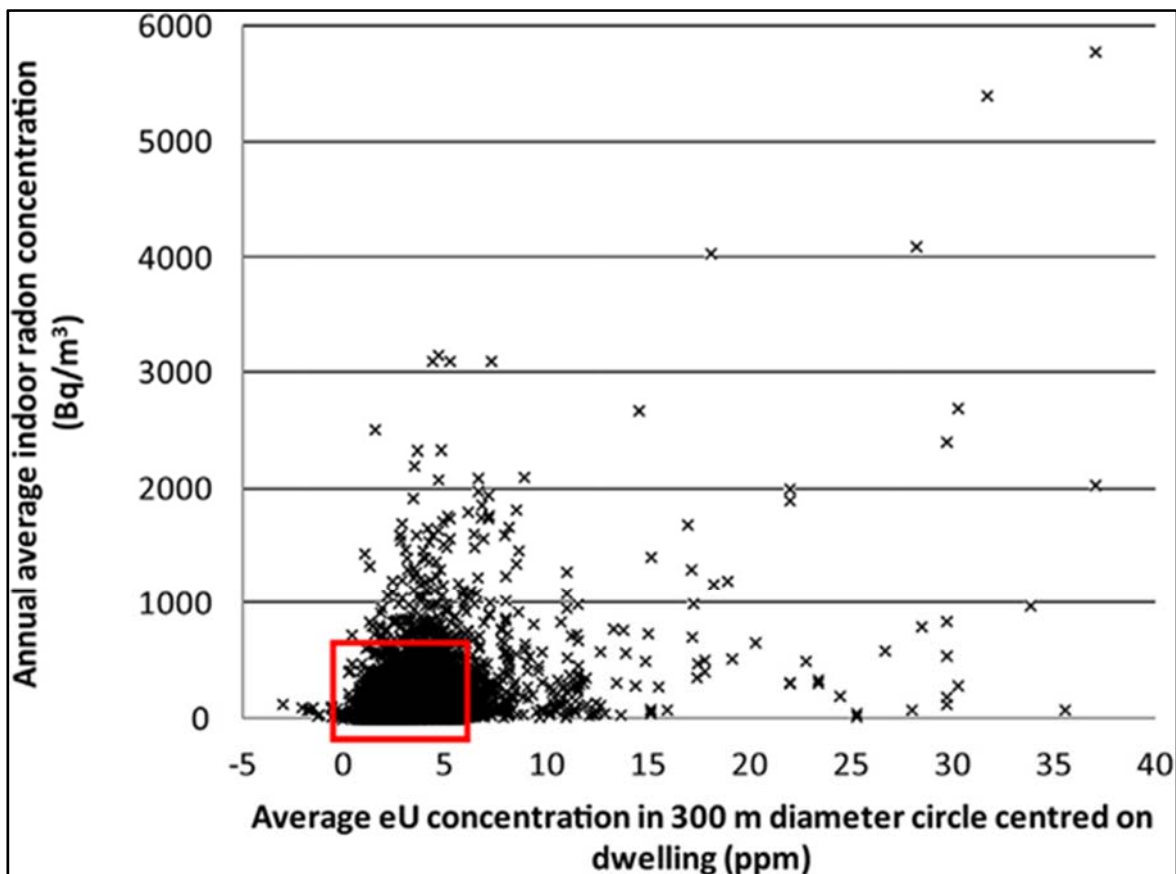
### 3. CONVERTING THE URANIUM GRID COMPILATION INTO A RADON HAZARD MAP

The source of radon is the natural existence of uranium in Norwegian bedrock and soils. The equivalent uranium (eU) concentrations in parts per million (ppm) can be regarded as relative radon concentrations in the near surface of the ground.

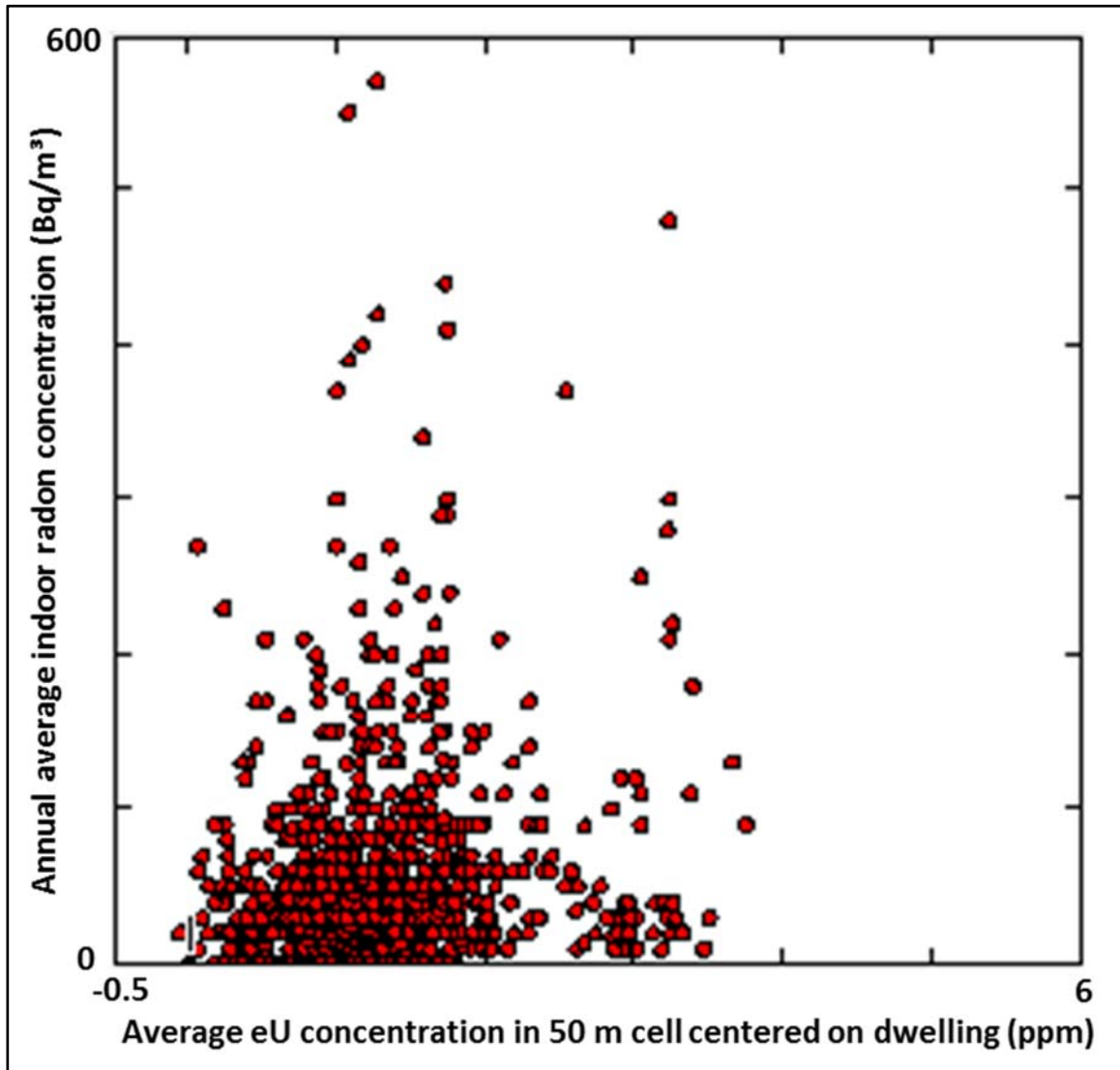
The eU map of the Trøndelag area is based on 12 airborne gamma ray spectrometer surveys that covers a large territory of the county. Airborne geophysical surveys have been and should resume to be a part of the regional mapping of Norway. These measurements reveal a good summary of the ground eU concentration regardless of the bedrock or sediment origins.

Earlier studies, in the Oslo area, have revealed the correlation among the indoor radon concentrations equal to or above 200 Bq/m<sup>3</sup> (RP200), the airborne gamma ray eU map and geological map (Smethurst et al., 2017).

These investigations have indicated that the eU model can account for approximately 70% of the variation in RP200, while the geologically controlled model accounts for around 40% of the variation in RP200. In this respect we consider airborne gamma ray survey eU data to be better than mapped geology at accounting for and therefore predicting differences in radon potential across the Oslo area.



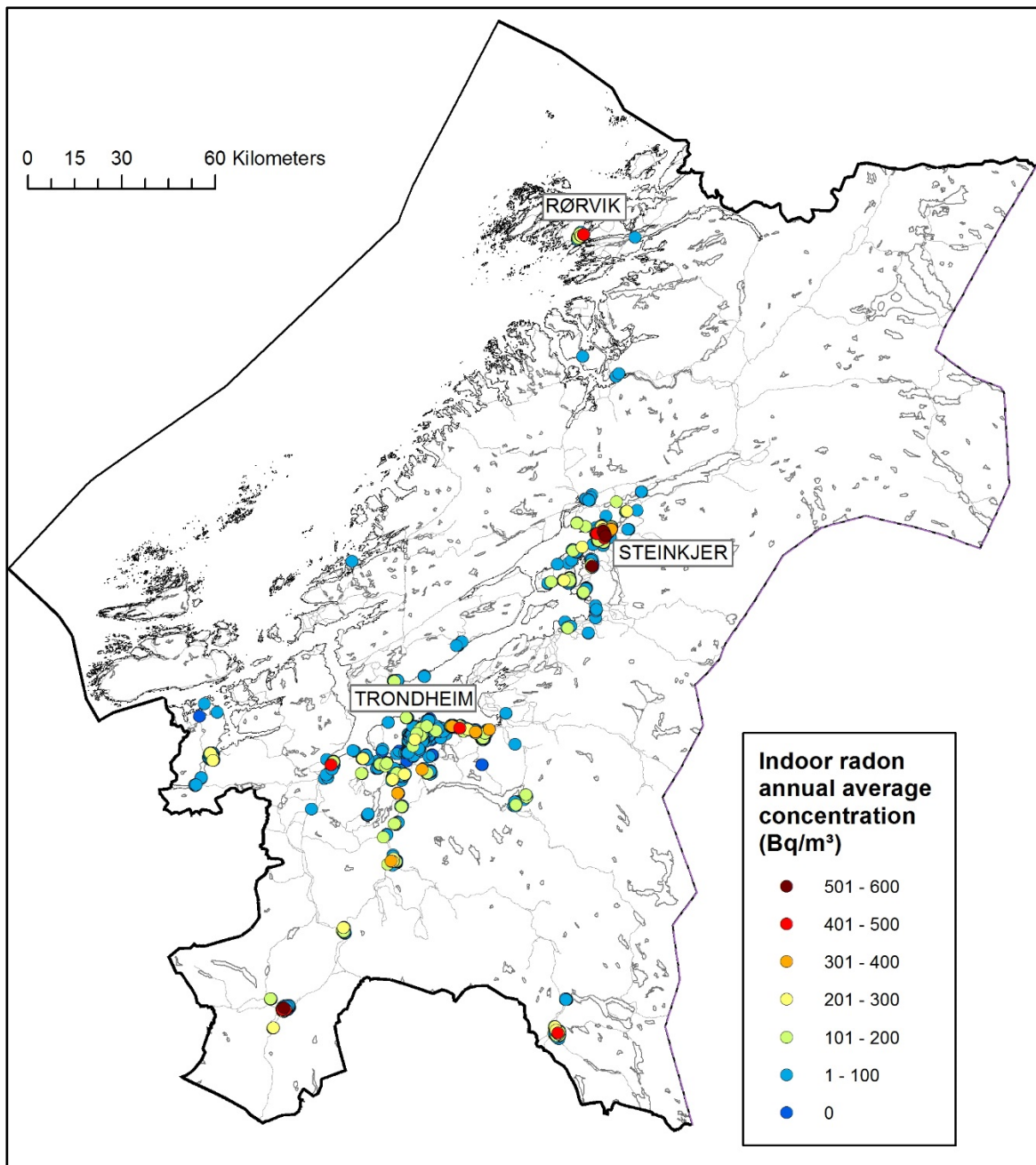
Figur 20. The relationship between annual average indoor radon concentration measurements and eU concentrations in the ground around dwellings in the Oslo area (Smethurst et al., 2017). Red square indicating Trøndelag data spread, is shown in detail in Figure 21.



Figur 21. The relationship between annual average indoor radon concentration measurements and eU concentrations in the ground around dwellings in the Trøndelag area.

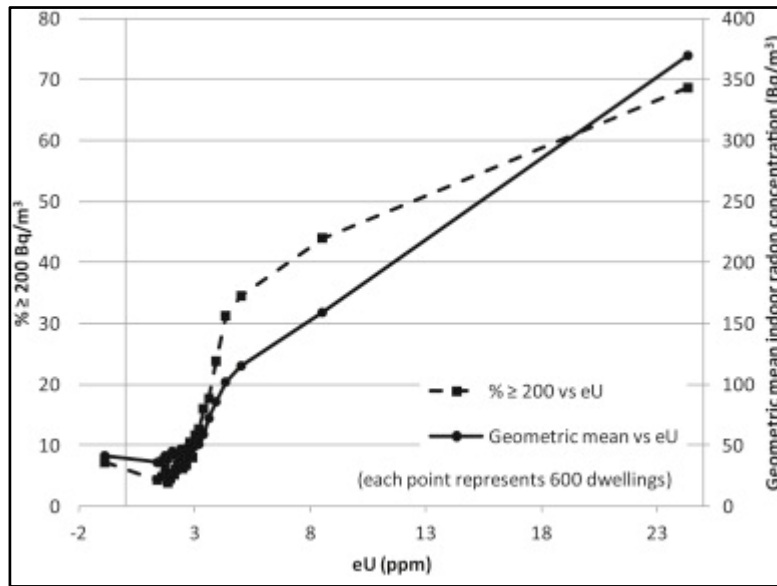
Figure 21 shows that the relations between annual average indoor concentration measurements and eU concentrations in the ground around dwellings in the Trøndelag area resemble parts of the relations in the Oslo region (Fig. 20).

In the Trøndelag area there are 1,366 indoor concentration measurements that have mutual coordinates with eU grid cells. Figure 22 shows the selected points' position in a map. Most measurements are concentrated around the towns of Trondheim, Steinkjer and Rørвик. The colors of the symbols indicate the dwellings' annual average indoor radon concentrations. The symbols are drawn in an ascending order on the map, so that symbols representing the highest radon concentrations are brought to front. The major part of the Trøndelag area has no indoor radon concentration measurements. It is therefore hard to make a reliable radon risk map for the whole county based on the available indoor recordings.

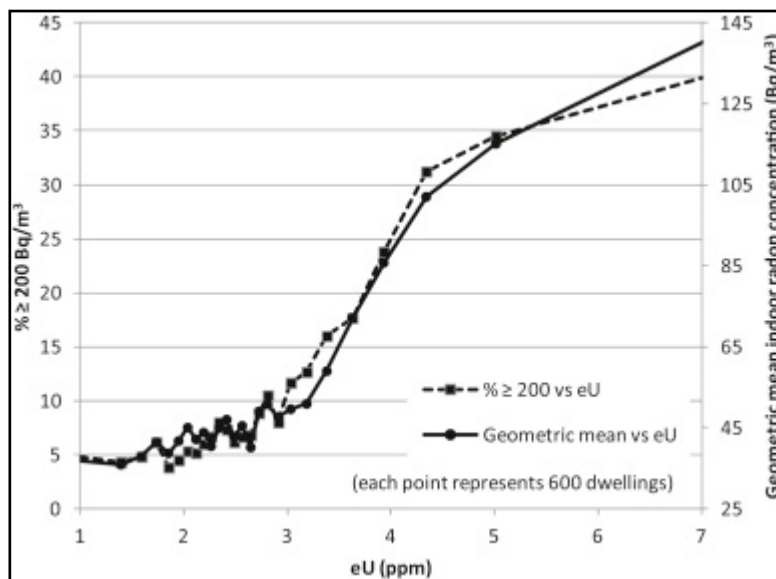


Figur 22. Dwellings with indoor radon annual average concentrations (Bq/m<sup>3</sup>).

The percentages of Oslo area dwellings with indoor radon concentrations equal to or above 200 Bq/m<sup>3</sup> (RP200), as well as the geometric mean indoor radon concentrations, are plotted against eU values in Figure 23. The plot, enlarged in Figure 24, shows a very systematic increase in RP200, and geometric mean, with increasing eU concentration in the Oslo area.



Figur 23. Oslo region radon potential ( $\% \geq 200 \text{ Bq/m}^3$ ) and geometric mean of indoor radon concentration as functions of eU concentration in the ground (Smethurst et al., 2017).

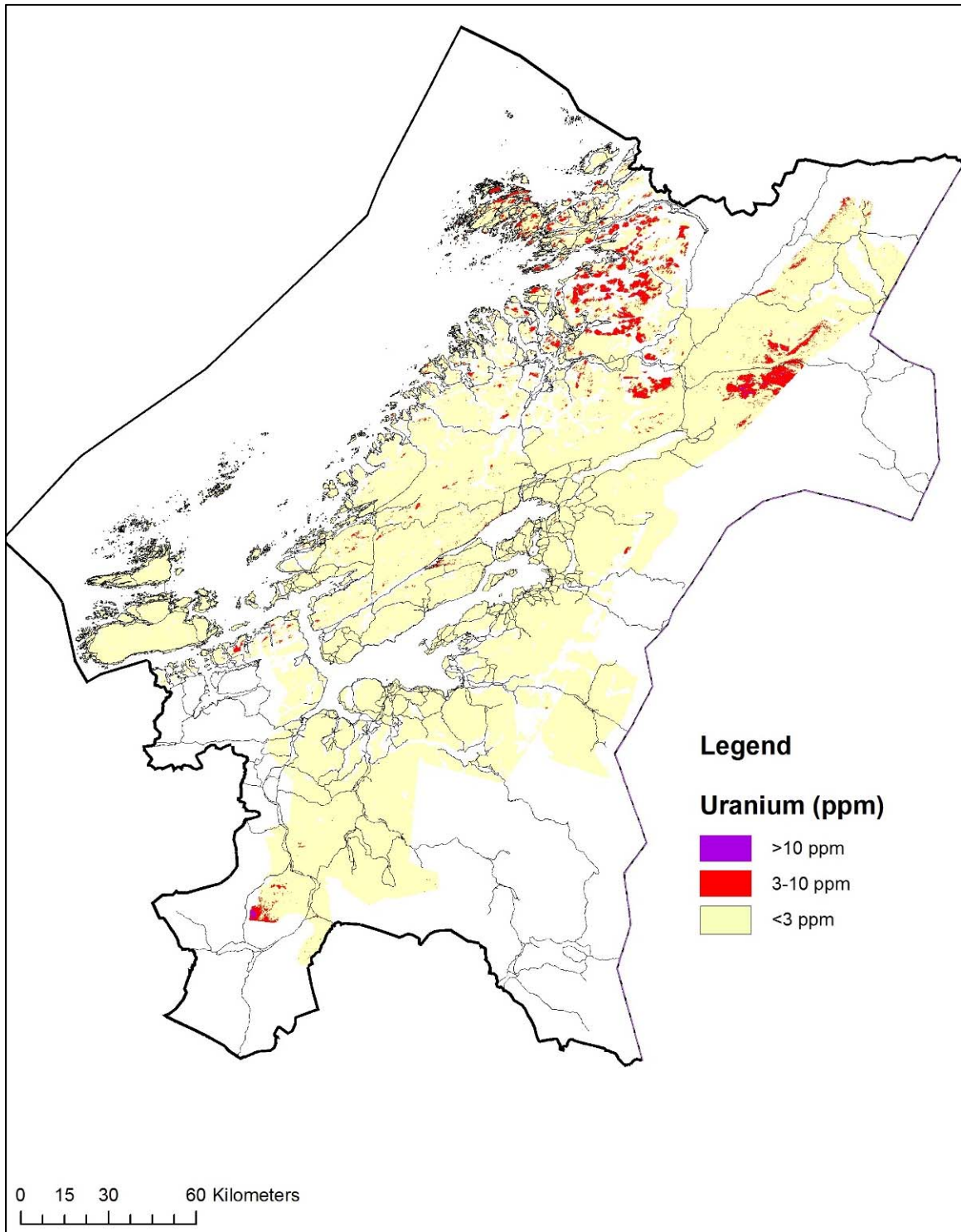


Figur 24. Re-scaled enlargement of Figure 23 between 1 and 7 ppm eU (Smethurst et al., 2017).

There is almost a one hundred times larger number of indoor radon measurements in the Oslo Fjord survey area (120,880 measurements) compared to the Trøndelag survey area (1,366 measurements). We therefore maintained the statistics from the Oslo region. Based on the Oslo region correlations (Smethurst et al., 2017) we have used the following graduation of eU concentration in the ground (ppm) and radon hazard when introducing a radon map for Trøndelag.

- > 10 ppm, very high radon hazard
- 3-10 ppm, high radon hazard
- < 3 ppm, moderate to low radon hazard

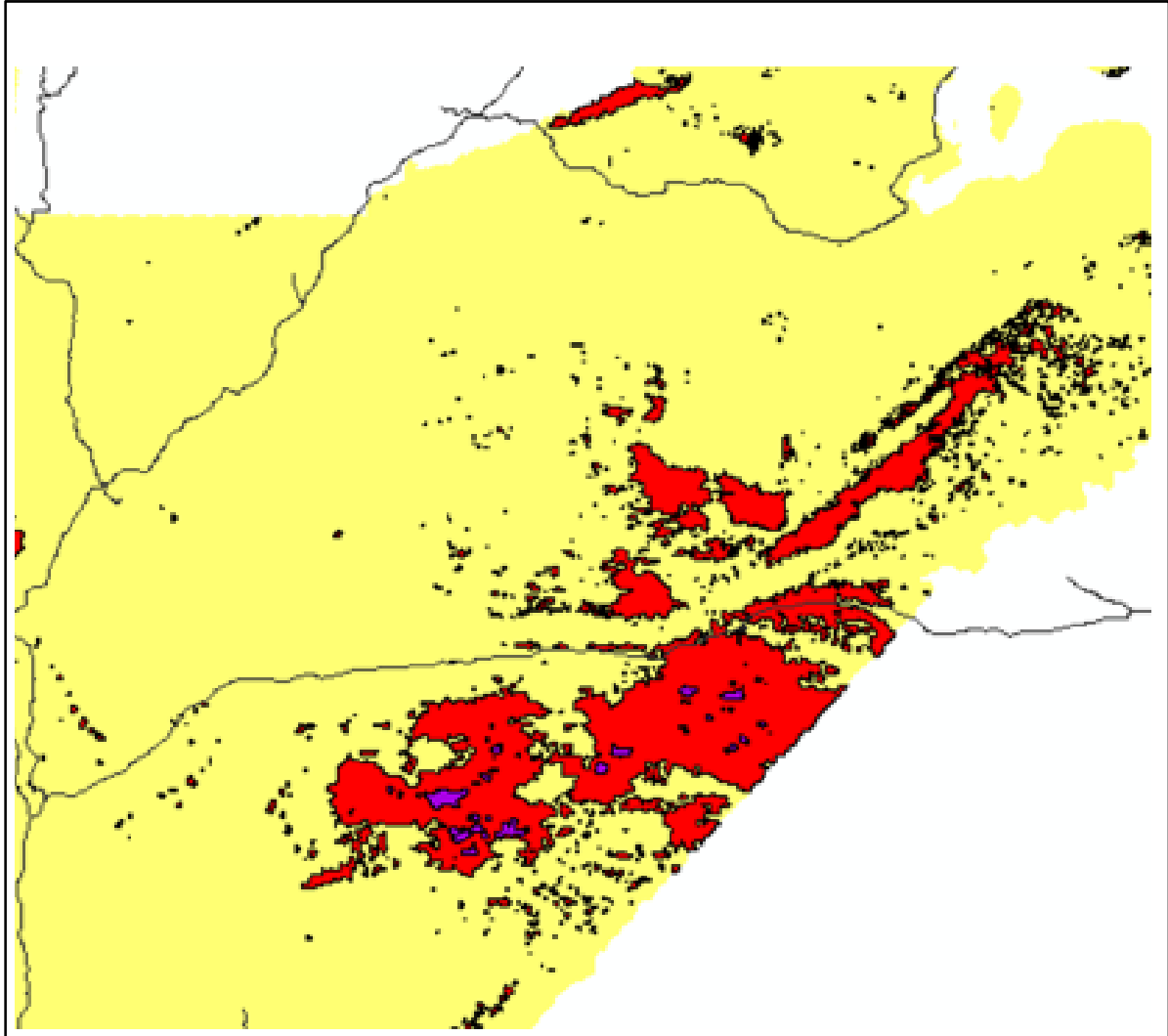
Figure 25 presents the uranium grid values as graduations based on these three classifications.



Figur 25. The graduation of eU (ppm) in three classifications based on fixed-wing and helicopter measurements over the Trøndelag county.

Because the aircraft moves forward during the accumulation time, the area of ground sampled is elongated. A rule of thumb indicates that 60-70% of the counts originate in a rectangle with a width of twice the flying altitude, and a length of twice the flying altitude plus the distance travelled during

accumulation. For a typical fixed-wing survey, at an altitude of 60 m, a speed of 225 km/h and accumulation time 0.5 s, the area represented by each sample is about 120 m x 150 m. Thus, airborne surveys normally result in lower uranium values, because they represent average contributions from a variety of radioactive sources. Local ground variations will therefore be smoothed.



*Figur 26. A segment of the classification map from the Grong area.*

Figure 26 shows a segment of the eU classification map. The map is apparently detailed, due to the fact that each measuring value, that represents an average of 18,000 square meter, is plotted in the center of this rectangle.

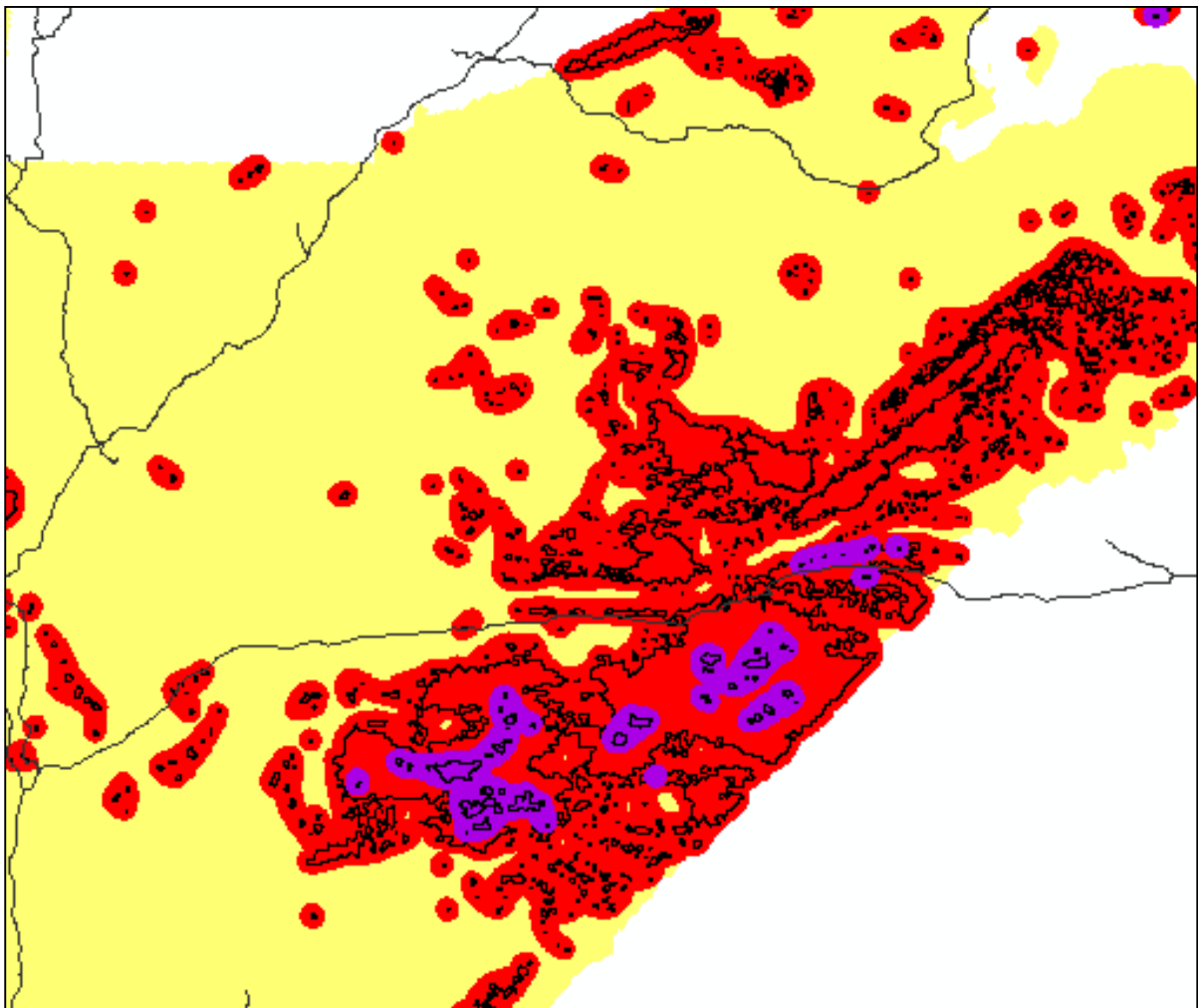
We used Arc Toolbox (ArcGIS Desktop 10.6) to improve the dataset by reducing its apparent resolution and to expand the anomalous polygons.

Aggregate Tool:

This tool combines polygons within a specified distance of each other into new polygons. It is intended for moderate scale reduction and aggregation when one do not want input features to be represented individually due to the required data resolution. Aggregation will only happen where two polygon boundaries are within the specified aggregation distance to each other. In this case we sat the aggregation distance to 1,000 meters.

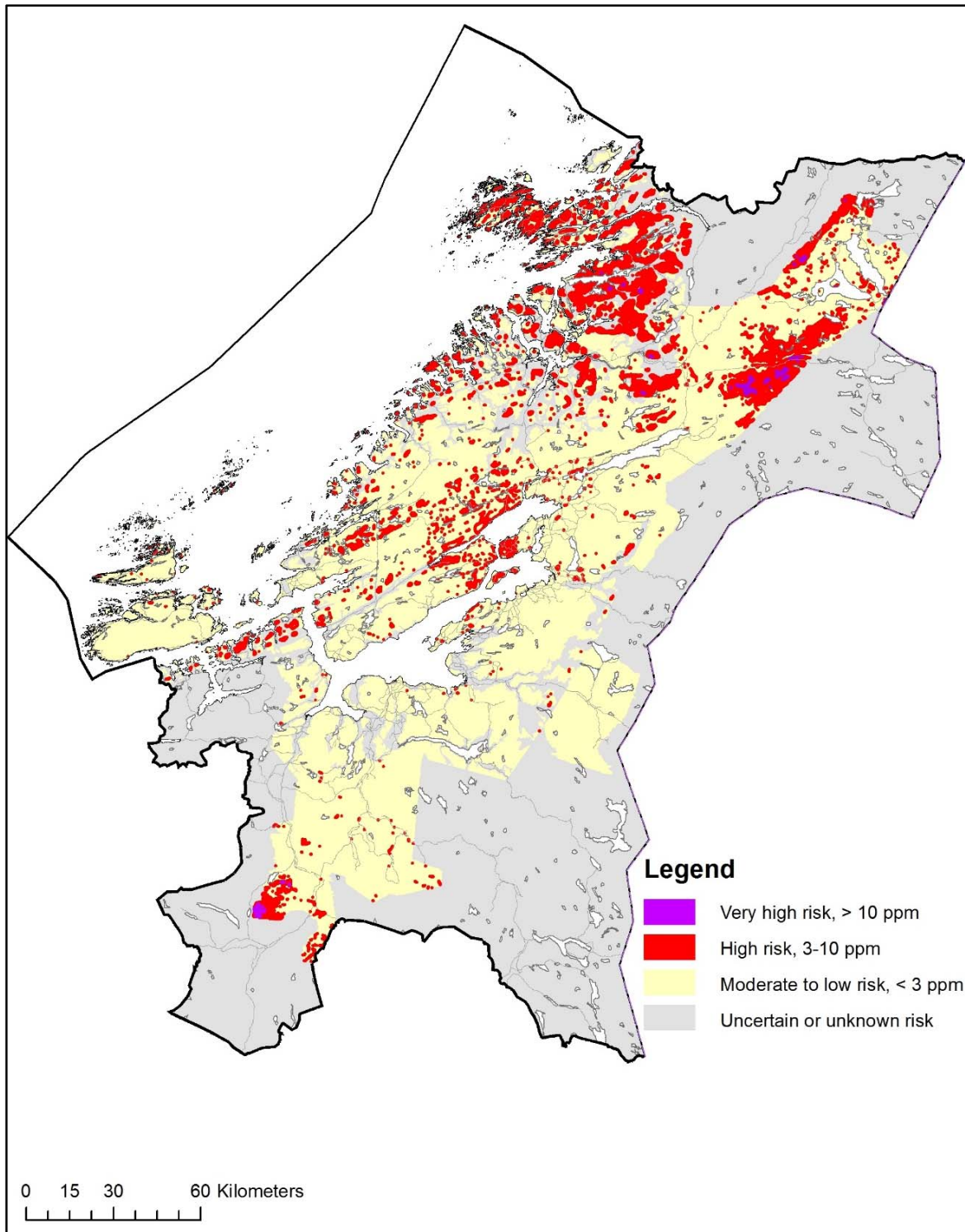
Buffer Tool:

This tool creates buffer polygons around input features to a specified distance. In this case we used the Buffer Tool to define an area within the distance of 500 meters around the input anomalies.



*Figur 27. The segment map in Figure 26 after aggregation (1000 m) and buffering (500 m) of anomaly classification polygons.*

Figure 28 shows aggregated and buffered ground concentrations of uranium and their equivalent radon risk potentials.

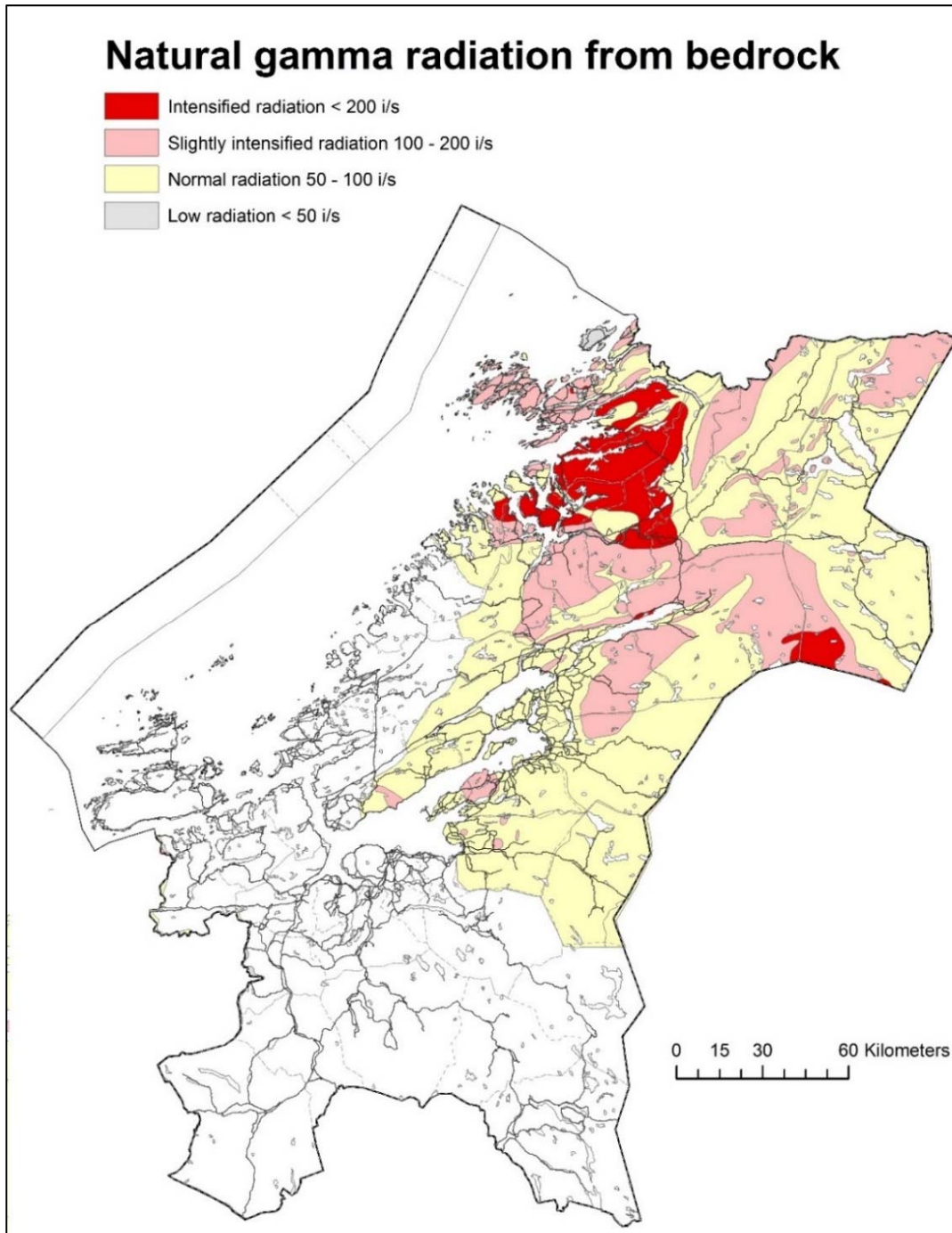


Figur 28. Estimated ground concentration of uranium with aggregation distance of 1000 m and buffer distances of 500 m. The graduation of eU (ppm) and radon risk are presented in 4 classifications.

Areas with no fixed-wing or helicopter measurements are classified as uncertain or unknown hazard. In those areas we may use other data to identify sites which are likely to be exposed to elevated radon concentrations. One of these datasets are the ground measurements of natural total gamma radiation performed with scintillometer from 1975 to 1992.

### 3.1 GAMMA RADIATION GROUND MEASUREMENTS

The natural radioactivity measurements that gives foundation to this map were carried out from 1975 to 1992. The total gamma radiation map (Lindahl et al., 1996) shows natural radiation from bedrock, interpreted from a combination of ground measurements, along all main roads, and bedrock maps (Figure 29).



Figur 29. Total gamma radiation, measured with scintillometer along roads in Trøndelag county (Lindahl et al., 1996).

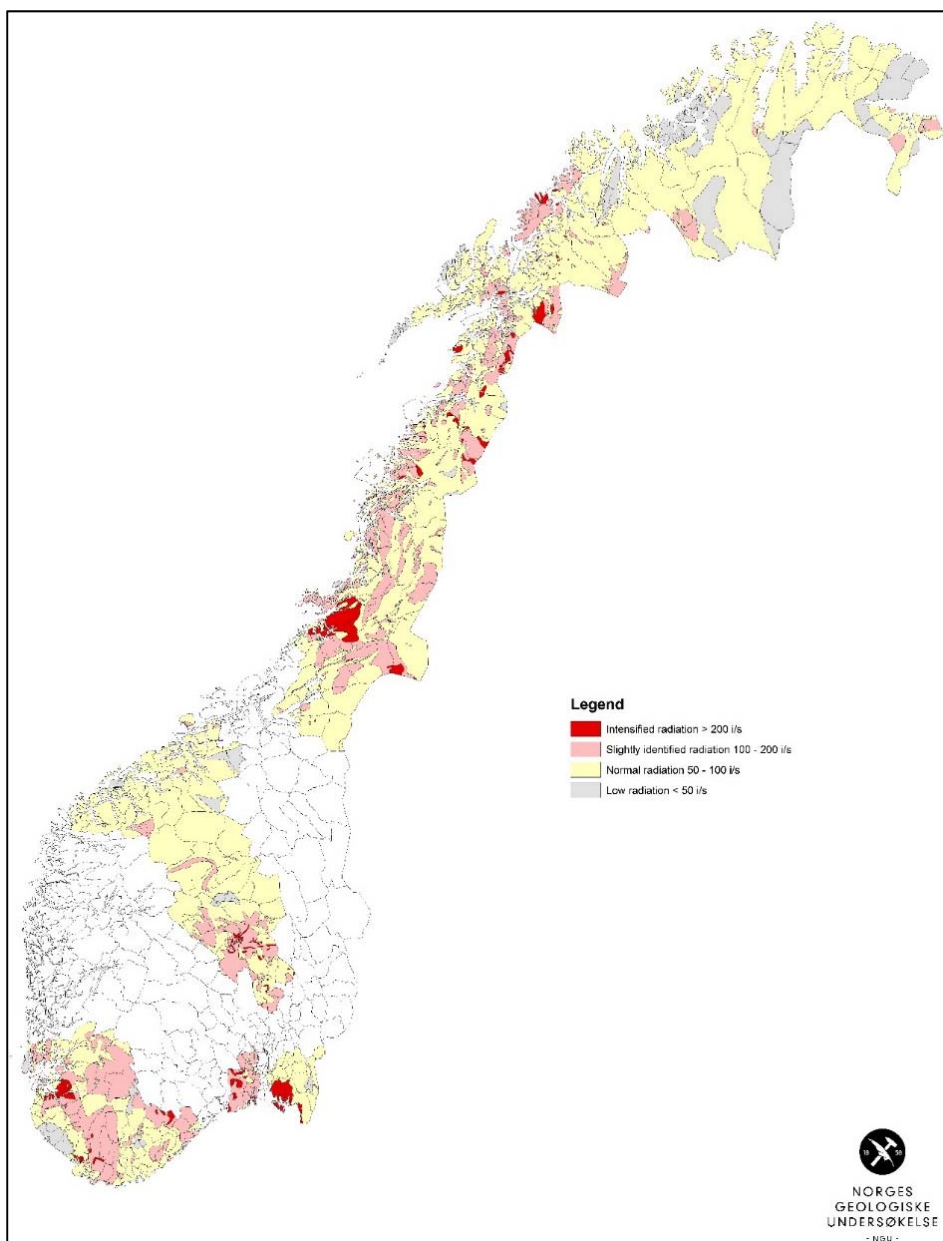
The map shows variation of total gamma radiation mainly measured on bedrock outcrops along the roads. The measurements are performed with a calibrated scintillometer. The values have the denomination of pulses per second (i/s), referred to as Saphymo SRAT no. 1, anno 1976. The main

part of the measured radioactivity is the result of decomposition of uranium, thorium and potassium that exist naturally in the bedrock.

These results can be regarded as a substitute to the airborne radiation measurements, and may be useful in areas where we still do not have data from fixed-wing or helicopter surveys. This map identifies areas which are likely to be exposed to elevated radon concentrations.

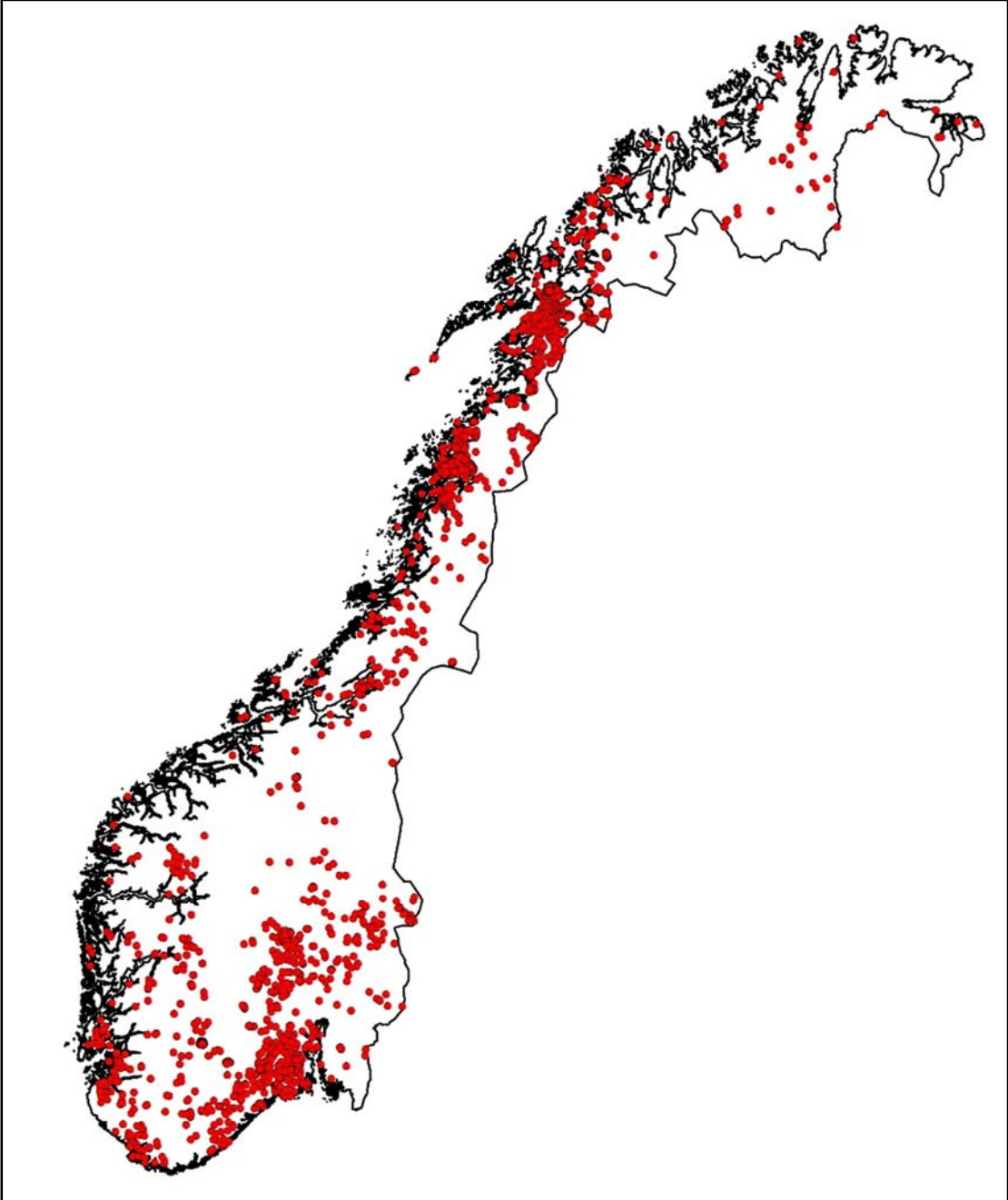
The uncolored areas represent counties where supplementary measurements should be performed to improve the coverage. Still we have used some of the draft data in those white areas when preparing the final radon hazard map of the Trøndelag county.

Figure 30 shows a collocation of county maps, produced so far, from natural gamma radiation measured on bedrock. This map may be useful as supplementary information when producing a national radon hazard map.



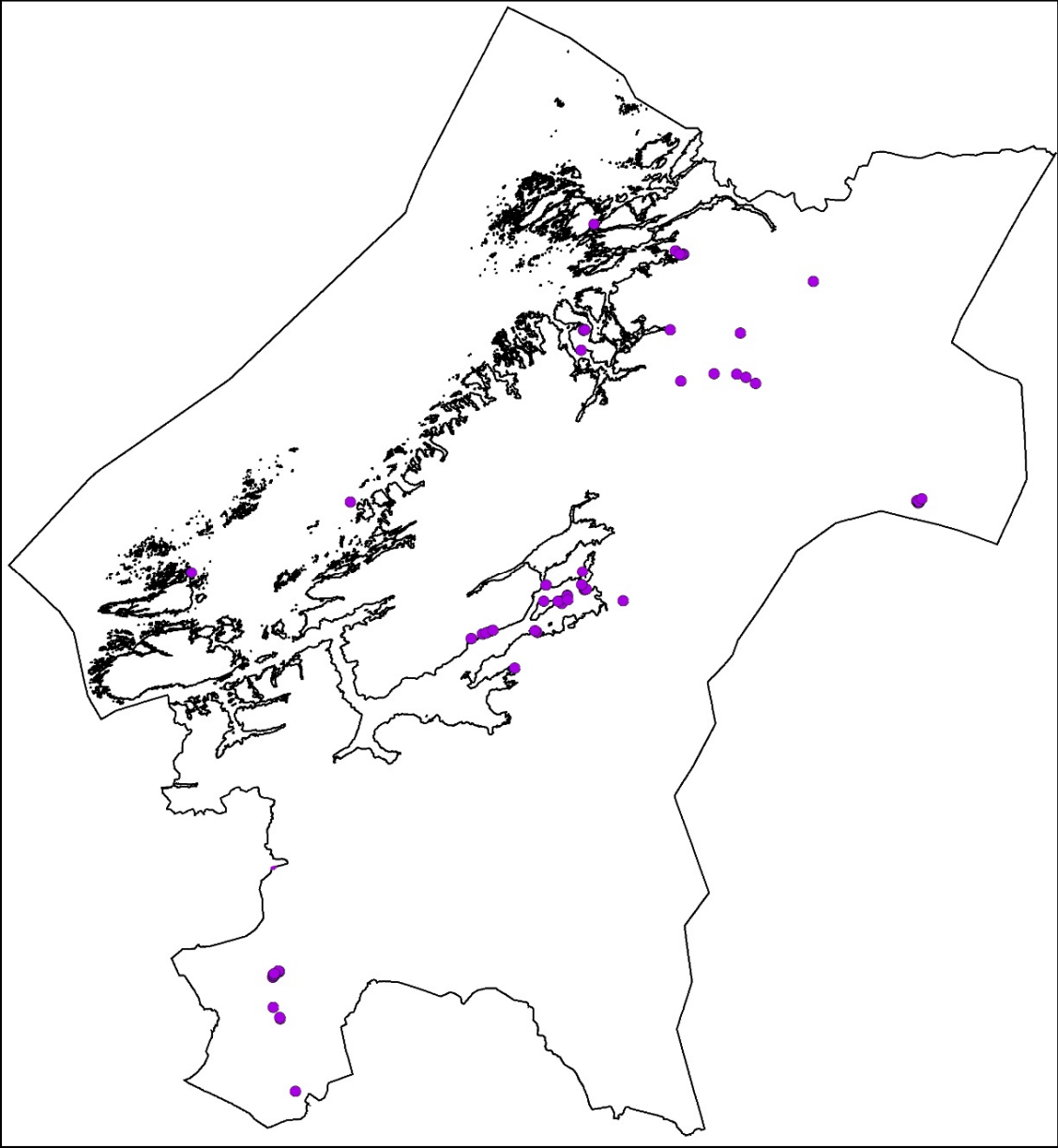
Figur 30. Interpretation map of natural gamma radiation from bedrock. This map may identify areas which are likely to be exposed to elevated radon concentrations (Lindahl et al., 1996).

Based on scintillometer measurements, bedrock samples were collected from anomalous sites for supplementary XRF analyses. These XRF analytical results reside in the NGU URANAL database (Figure 31).



Figur 31. Distribution of bedrock samples in the URANAL database.

The detection limit for XRF analyses is approximately 10 ppm for uranium, so there are no low measured uranium variables in the URANAL database. After all, the objective of the XRF analyses is to trace deposits of high uranium concentrations.



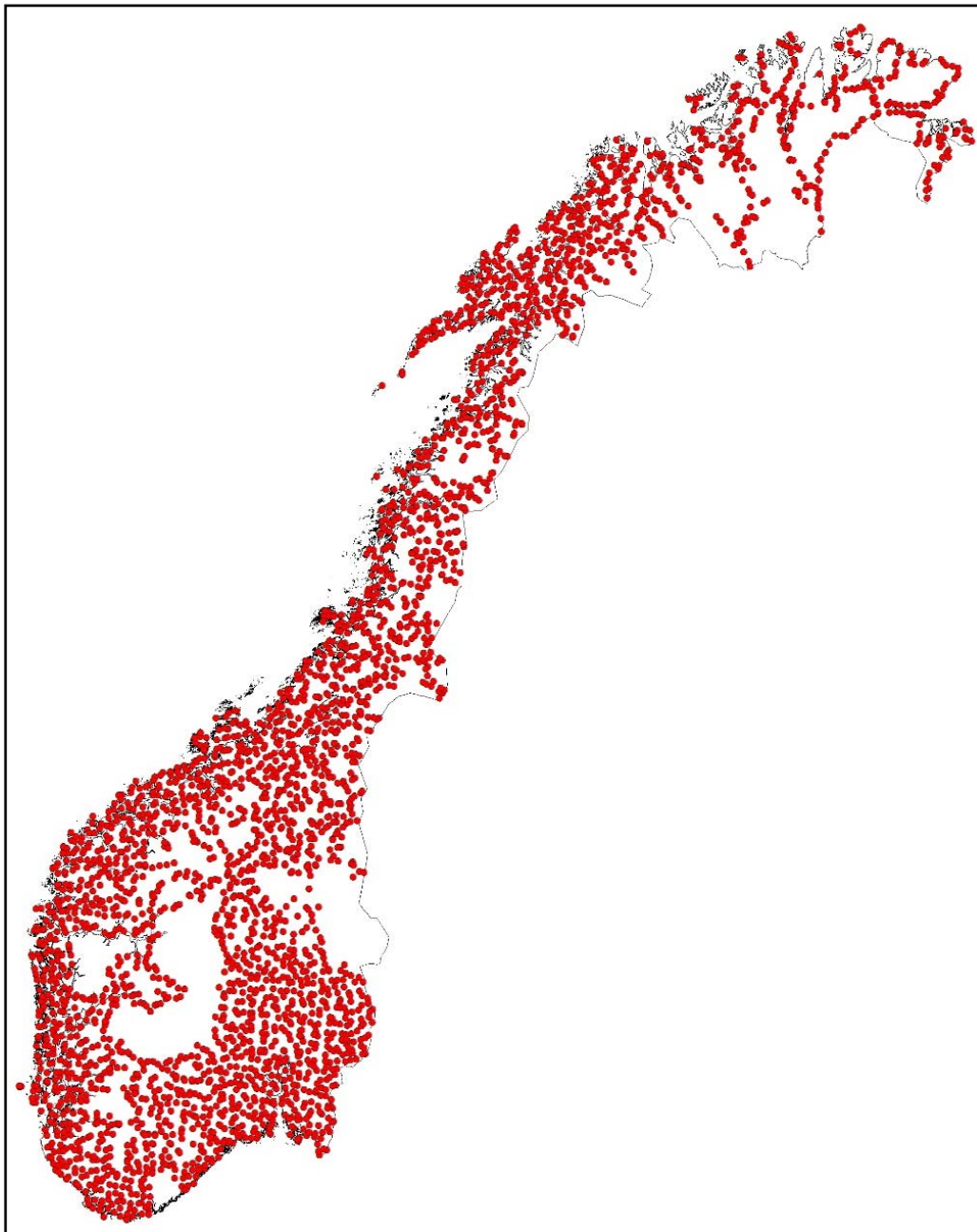
Figur 32. Distribution of XRF analysed bedrock samples from the URANAL database, with uranium content > 10 ppm, within the Trøndelag county.

### 3.2 GEOCHEMICAL COMPOSITION OF THE BEDROCK (LITO DATABASE)

The LITO database is another dataset that can be used to identify sites which are likely to be exposed to elevated radon concentrations.

The LITO project was initiated in 1999 and aimed at mapping chemical compositions and petro-physical characteristics of all mapped bedrock units in Norway.

The gathering of samples is based on the national geological maps at the scale of 1:250,000. To ensure a good geographic covering the country is divided into a 9 by 9 km network. One sample is collected within each square. The sample is taken from a 3 m long core to ensure fresh, un-weathered bedrock. Figure 33 shows the distribution of LITO samples up to 2017.

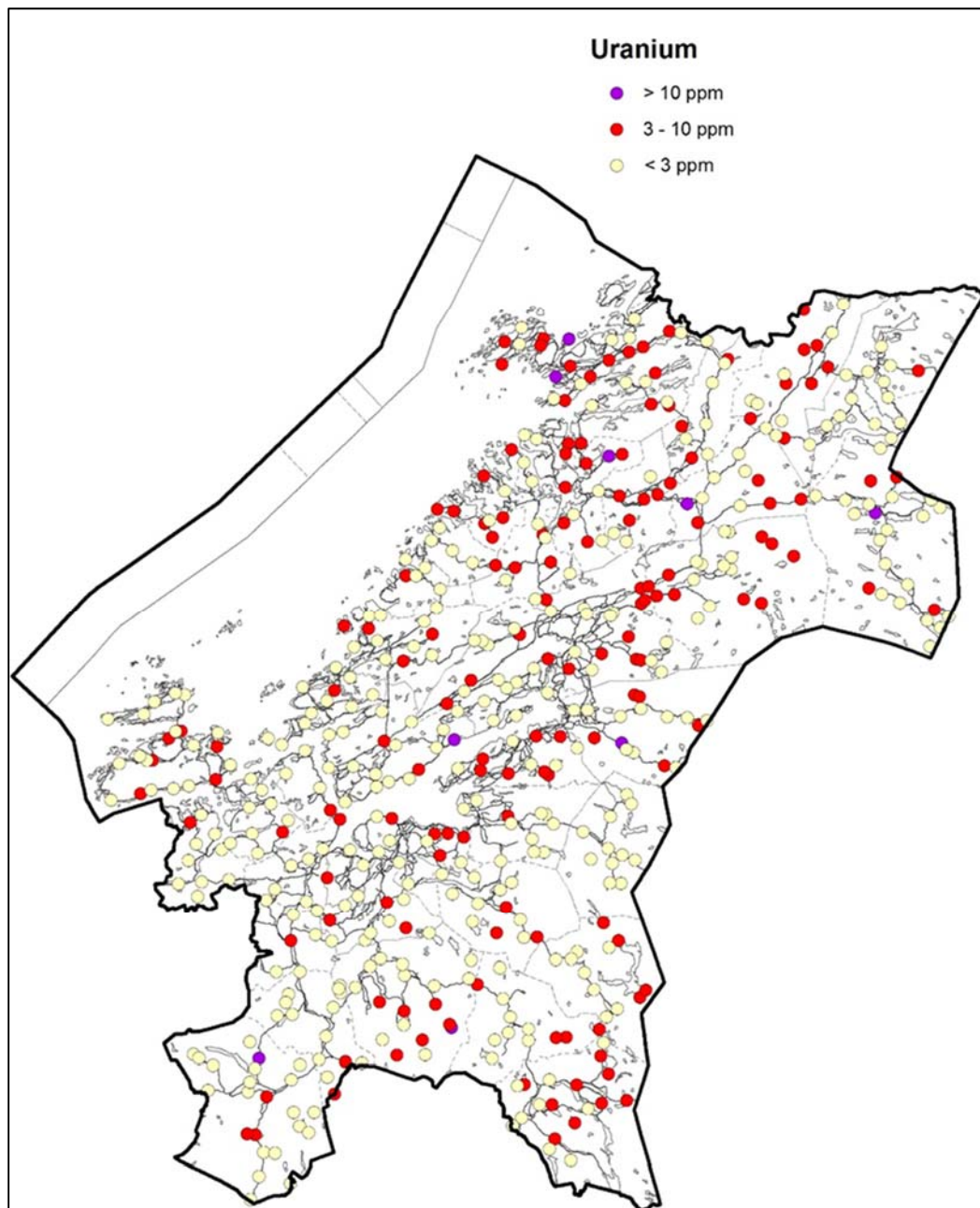


Figur 33. The distribution of LITO samples up to 2017.

The chemical analyses are carried out at NGU's laboratory to map major- and trace elements of the rock types. These analyses include X-ray fluorescence (XRF), Inductively coupled plasma mass spectrometry (LA-ICP-MS), Inductively coupled plasma atomic emission spectroscopy (ICP-AES) and atomic absorption.

Every fifth sample is analyzed in duplicate, and every tenth sample is a standard with known composition. This is done to insure quality of measuring results and to remove any instrumental drift. The final results are compiled in a very comprehensive geochemical and petrophysical national dataset.

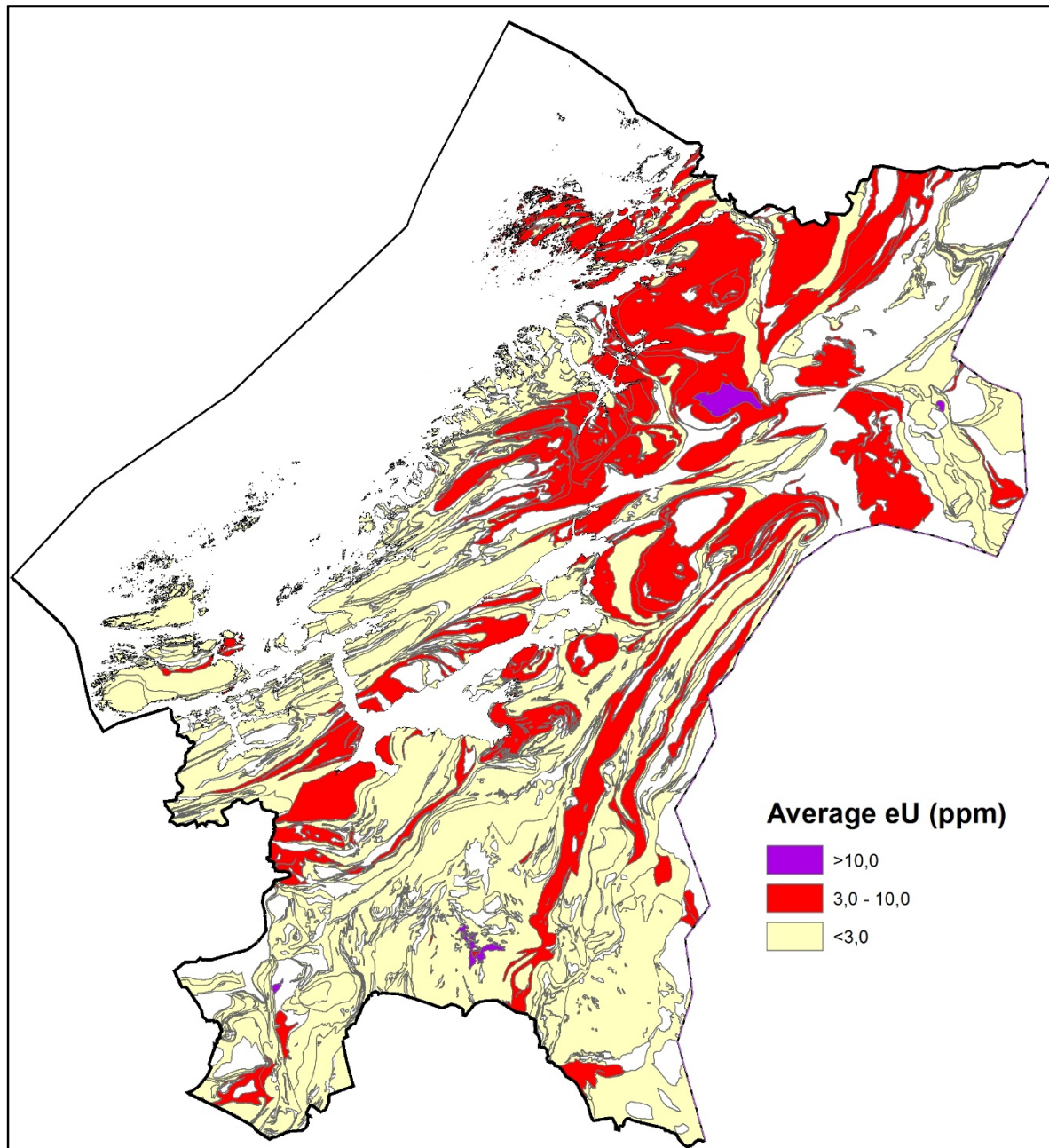
Figure 34 shows the uranium concentrations (ppm) for the LITO samples covering Trøndelag county.



Figur 34. Uranium concentrations in ppm for the LITO samples from Trøndelag.

The gradation of uranium content is presented in three classifications like the ones described in Chapter 3 and used in Figures 25 and 28.

Based on these LITO samples (Figure 34), we have produced a map of uranium content by calculating the average values within each geological unit present in the bedrock map of Trøndelag (Figure 35).



*Figur 35. Average uranium concentrations (ppm) calculated from LITO samples within each bedrock unit.*

This allows us to identify areas which can be exposed to elevated radon concentrations from bedrock although Quaternary deposits shield the natural radiation, and where we do not have airborne uranium measurements.

Thus, to cover the whole of Trøndelag county with estimates on radon hazard, we combined the maps from Figures 28 and 35. This gives an improved radon hazard map (Figure 36) derived from both airborne uranium measurements and from average geochemical uranium analyses of bedrock samples.

In some Quaternary areas, where the airborne measurements indicate moderate to low radon hazard, but with existing LITO bedrock samples containing more than 3 ppm uranium, one should rather use the average uranium calculation to describe the radon distribution. After all there is a radon hazard in these areas when excavating building sites reaching the bedrock.

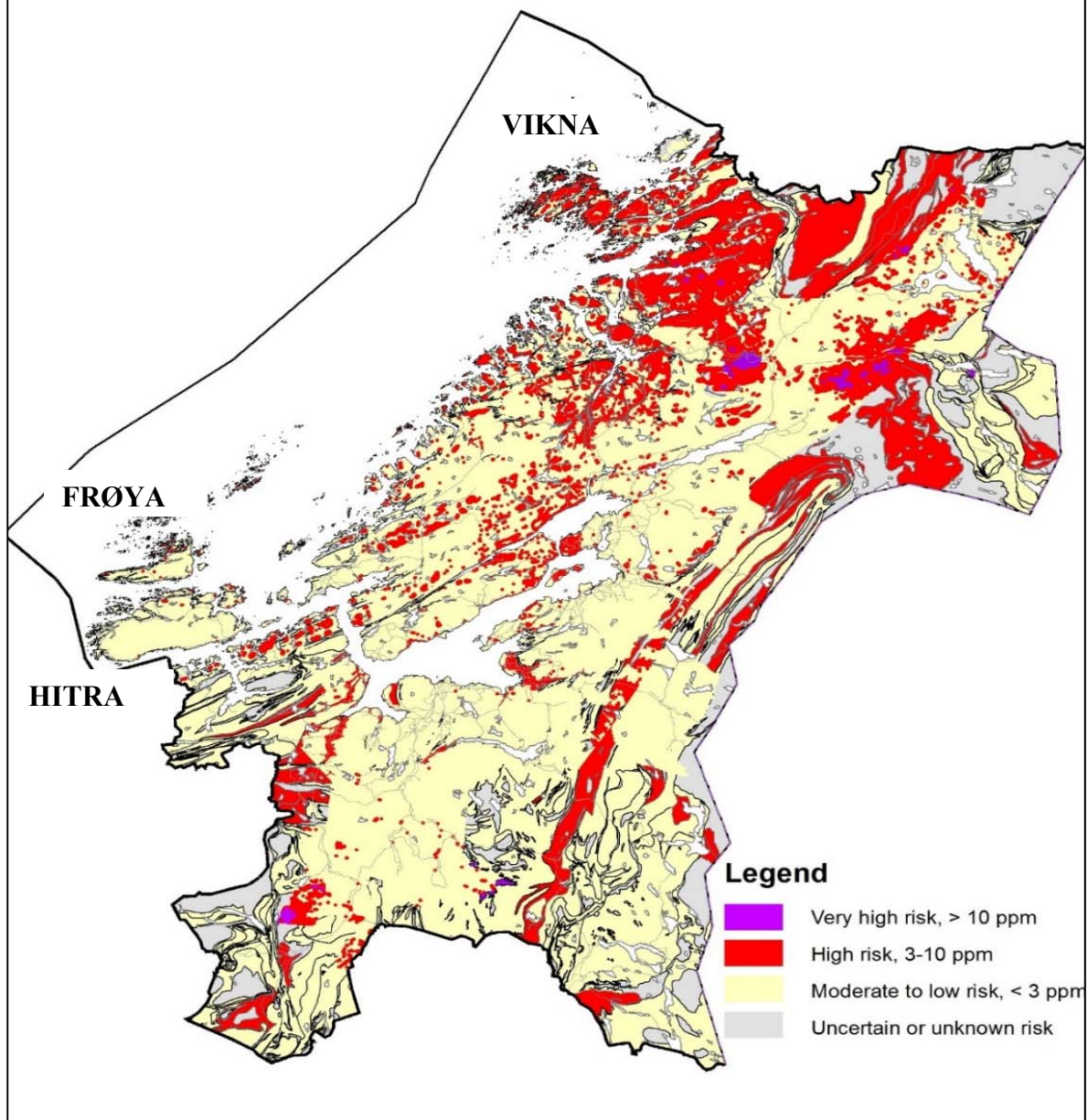
Compared to the present national radon hazard map (Figure 37) (Smethurst et al., 2014; Watson et al., 2017), based on indoor radon measurements and existing bedrock maps, and residing at <http://geo.ngu.no/kart/radon/>, this new and improved map is founded on real measurements and consequently on more reliable and consistent data. Thus, several areas appear different, in the two maps, when it comes to radon risk.

The two maps use slightly different colour scales but this does not cause the big location difference in high and low radon hazard areas. As an example, the improved radon hazard map shows the islands Frøya and Hitra standing out as “moderate to low” in contrast to “high” in the published map. In addition, the Vikna islands display as “high radon hazard” areas in the improved map, while they are defined as “moderate to low” in the existing map. There are also severe discrepancies between the two maps on the Fosen peninsula as well as in the eastern Trøndelag area. Similar differences can be seen between the existing radon hazard map and airborne eU maps in southern and northern Norway. The main shortcoming of the present radon hazard map is the extrapolation from dense indoor measurements in urban areas to rural areas with few or none measurements. Using the poorly constrained bedrock map without any connection to the uranium content for the extrapolation causes numerous errors. The uranium content of gneiss and granitoids as well as metasediments has a large variation as revealed by both airborne and laboratory measurements.

We consequently suggest producing a new national radon hazard map with the procedure outlined in the present report. The present erroneous and misleading map should be replaced by an improved map.

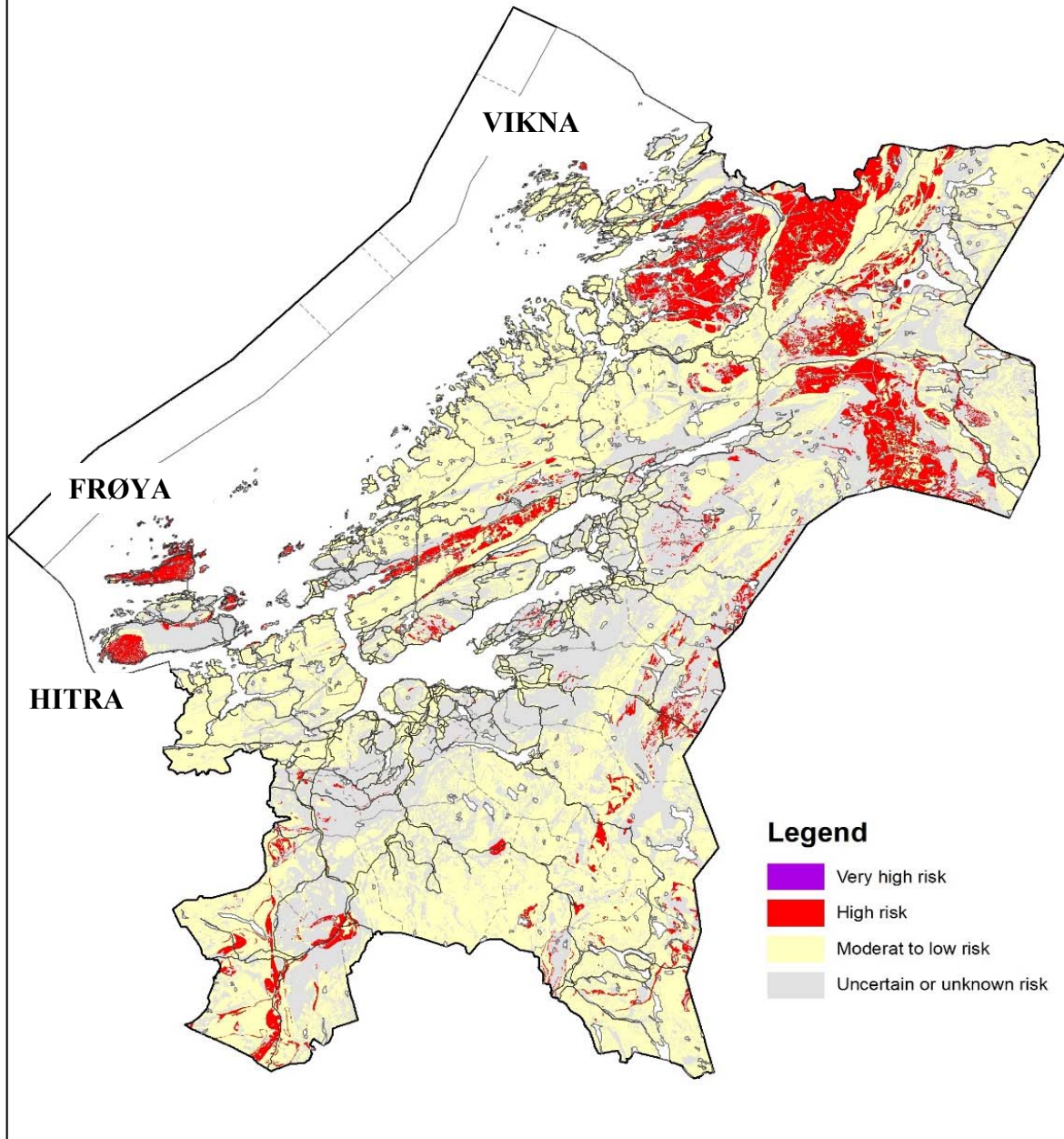
## Improved radon risk map, Trøndelag

Derived from airborne uranium measurements  
and geochemical analyses of bedrock samples



Figur 36. New national radon risk map – Trøndelag test area. The map is based on both airborne radiometric measurements as well as average geochemical analyses of bedrock samples (LITO project).

## Former radon risk map, Trøndelag <http://geo.ngu.no/kart/radon/>



Figur 37. Published former radon hazard map based on indoor radon measurements and existing bedrock maps, Trøndelag. (<http://geo.ngu.no/kart/radon/>), (Smethurst et. al., 2014).

## ***Acknowledgements***

Novatem from Mont-Saint-Hilaire in Québec carried out the TRAS-14 airborne survey. NGU, Oljedirektoratet, AkerBP, BKK, ConocoPhillips, DEA, Equinor, INEOS, Lundin Petroleum, Neptune, Noreco, Nye Veier, Repsol, Spirit Energy, Suncor, Total and Vår Energi funded the Coop1/2 Project. We express our sincere thanks to all these companies and institutions. Ingvild Engen Finne from the Norwegian Radiation and Nuclear Safety Authority provided indoor radon measurements and contributed with useful comments to the present report.

#### 4. REFERENCES

- Geosoft 2010: Montaj Geophysics Levelling System - Processing and Enhancing Geophysical Data Extension for Oasis montaj v7.1 - Tutorial and User Guide. Geosoft, 70 pp.
- Håbrekke, H. 1983: Geofysiske målinger fra helikopter over et område vest for Berkåk i Rennebu. NGU Report 2089, 16 pp.
- IAEA. 1991: Airborne Gamma Ray Spectrometer Surveying. Technical Reports Series 323, Vienna, Austria, 97 pp.
- Lindahl, I., Sørdal, T. & Ekremseter, J. 1996. Naturlig radioaktivitet fra berggrunnen, NORGE. M 1 : 2 000 000, Norges Geologiske Undersøkelse.
- Maystrenko, Y. 2013: 2D gravity, magnetic and thermal modelling near Bergen and Stavanger; a COOP Report. NGU Report 2013.059, 103 pp.
- Maystrenko, Y. 2014: 3D gravity, magnetic and thermal modelling within the northern North Sea and adjacent areas; a Coop Report, NGU Report 2014.026, 114 pp.
- Mogaard, J.O., Rønning, S., Blokkum, O. & Khile, O. 1989: Helikoptermålinger kartblad Steinkjer, Nord-Trøndelag. NGU Report 89.142, 30 pp.
- Mogaard, J.O. & Blokkum, O. 1993: Geofysiske målinger fra helikopter over Meråkerfeltet, Nord-Trøndelag. NGU Report 92.153, 9 pp.
- Novatem 2014: Fixed-wing magnetic and radiometric survey of the Trøndelag Region in Norway. C12095, Airborne survey for NGU, TRAS-12 Norway 2011-2014 project. Novatem internal report.
- Olesen, O., Brønner, M., Ebbing, J., Elvebakk, H., Gellein, J., Koziel, J., Lauritsen, T., Lutro, O., Maystrenko, Y., Müller, C., Nasuti, A., Osmundsen, P.T., Slagstad, T., & Storrø, G. 2013: COOP Phase I – Crustal Onshore-Offshore Project. NGU Report 2013.002, 361 pp.
- Olesen, O., Barnawal, V., Brønner, M., Dalsegg, E., Dumais, M.-A., Gellein, J., Gernigon, L., Heldal, T., Larsen, B.E., Lauritsen, T., Lutro, O., Maystrenko, Y., Nasuti, A., Roberts, D., Rueslåtten, H., Rønning, J.S., Slagstad, T., Solli, A. & Stampolidis, A. 2015: Coop Phase 2 Crustal Onshore-Offshore Project. NGU Report 2015.063, 410 pp.
- Rønning, S., Kihle, O., Blokkum, O. & Håbrekke, H. 1990: Helikoptermålinger kartblad GRONG og sydlige halvpart av kartblad HARRAN. NGU Report 89.085, 22 pp.
- Rønning, S. 1991: Helikoptermålinger over kartblad Andorsjøen, 1823 I. NGU Report 91.153, 14 pp.
- Rønning, S. 1992a: Helikoptermålinger over kartblad 1823 III, Snåsa. NGU Report 92.144, 13 pp.
- Rønning, S. 1992b: Helikoptermålinger over kartblad 1723 II, Snåsavatnet. NGU Report 92.145, 13 pp.
- Rønning, S. 1992c: Helikoptermålinger over kartblad 1723 I, Overhalla. NGU Report 92.146, 13 pp.
- Rønning, S. 1995a: Helikoptermålinger over kartblad 1722 IV, Stiklestad. NGU Report 93.084, 13pp.
- Rønning, S. 1995b: Helikoptermålinger over Grongfeltet, Nord-Trøndelag 1993 og 94. NGU Report 95.057, 14 pp.
- Rønning, S. 1995c: Helikoptermålinger over Fossenhalvøya, kartbladene 1622 I-IV og 1623 II og III. NGU Report 95.064, 19 pp.
- Skilbrei, J.R., 1993: Helikoptermålinger i Vuku-området, Steinkjer og Verdal kommuner, Nord-Trøndelag. NGU Report 93.104, 18 pp.
- Smethurst, M.A., Watson, R.J., Ganerød, G., Finne, I. & Rudjord, A.L. 2014. Nasjonalt aktsomhetskart for radon. M 1:1.000.000 NORGE. Utgitt av Norges geologiske undersøkelse i samarbeid med Statens strålevern.
- Smethurst, M.A., Watson, R.J., V.C. Baranwal., Rudjord, A.L. & Finne, I. 2017: The predictive power of airborne gamma ray survey data on the locations of domestic radon hazards in Norway: A strong case for utilizing airborne data in large-scale radon potential mapping. *Journal of Environmental Radioactivity* 166, (2017) 321-340.
- Watson, R.J., Smethurst, M.A., Ganerød, G.V., Finne, I. & Rudjord, A.L. 2017: The use of mapped geology as a predictor of radon potential in Norway. *Journal of Environmental Radioactivity* 166, 341-354.

[http://www.ngu.no/upload/Aktuelt/Produktark\\_RadonAktsomhet.pdf](http://www.ngu.no/upload/Aktuelt/Produktark_RadonAktsomhet.pdf)

<http://www.ngu.no/no/tm/Om-NGU/Prosjekter/Lito-prosjektet/Provetakiganalysen/>



GEOLOGICAL  
SURVEY OF  
NORWAY

· NGU ·

Geological Survey of Norway  
PO Box 6315, Sluppen  
N-7491 Trondheim, Norway

Visitor address  
Leiv Eirikssons vei 39  
7040 Trondheim

Tel (+ 47) 73 90 40 00  
E-mail [ngu@ngu.no](mailto:ngu@ngu.no)  
Web [www.ngu.no/en-gb/](http://www.ngu.no/en-gb/)